

**Diversity dynamics of Phanerozoic terrestrial tetrapods at the local-  
community scale**

Roger A. Close<sup>1</sup>, Roger B. J. Benson<sup>2</sup>, John Alroy<sup>3</sup>, Anna K. Behrensmeyer<sup>4</sup>, Juan Benito<sup>1,5</sup>,  
Matthew T. Carrano<sup>4</sup>, Terri J. Cleary<sup>1,6</sup>, Emma M. Dunne<sup>1</sup>, Philip D. Mannion<sup>7</sup>, Mark D.  
Uhen<sup>8</sup>, Richard J. Butler<sup>1</sup>

<sup>1</sup>School of Geography, Earth and Environmental Sciences, University of Birmingham,  
Edgbaston, Birmingham B15 2TT, UK.

<sup>2</sup>Department of Earth Sciences, University of Oxford, Oxford OX1 3AN, UK.

<sup>3</sup>Department of Biological Sciences, Macquarie University, NSW 2109, Australia.

<sup>4</sup>Department of Paleobiology, National Museum of Natural History, Smithsonian Institution,  
Washington DC 20013, USA.

<sup>5</sup>Department of Biology and Biochemistry, Faculty of Science, University of Bath, Claverton  
Down, Bath BA2 7AY, UK.

<sup>6</sup>Department of Earth Sciences, Natural History Museum, Cromwell Road, London SW7  
5BD, UK.

<sup>7</sup>Department of Earth Science and Engineering, Imperial College London, London SW6 2AZ,  
UK.

<sup>8</sup>Department of Atmospheric, Oceanic, and Earth Sciences, George Mason University,  
Fairfax, VA 22030, USA.

22   **The fossil record provides one of the strongest tests of the hypothesis that diversity**  
23   **within local communities is constrained over geological timescales. Constraints to**  
24   **diversity are particularly controversial in modern terrestrial ecosystems, yet long-term**  
25   **patterns are poorly understood. Here we document patterns of local richness in**  
26   **Phanerozoic terrestrial tetrapods using a global dataset comprising 145,332 taxon**  
27   **occurrences from 27,531 collections, much larger than that used any previous study. We**  
28   **show that local richness of non-flying terrestrial tetrapods has risen asymptotically**  
29   **since their initial colonization of land, increasing at most three-fold over the last 300**  
30   **million years. Statistical comparisons support phase-shift models, with most increases in**  
31   **local richness occurring: 1) during the colonization of land by vertebrates, concluding**  
32   **by the late Carboniferous, and 2) across the Cretaceous/Palaeogene boundary.**  
33   **Individual groups such as mammals, lepidosaurs and dinosaurs also experienced early**  
34   **increases followed by periods of stasis often lasting tens of millions of years. Mammal**  
35   **local richness abruptly tripled across the Cretaceous/Palaeogene boundary, but did not**  
36   **increase over the next 66 million years. These patterns are consistent with the**  
37   **hypothesis that diversity is constrained at local community scales.**

38

39       There is substantial disagreement about how the exceptional diversity of terrestrial  
40   life was assembled over geological time<sup>1-7</sup> and the macroevolutionary importance of  
41   processes observed in ecological communities<sup>6,8</sup>. In particular, studies of the fossil record  
42   have been central to debates about models of diversification and community dynamics on  
43   geological timescales<sup>8</sup>, but nominally global and regional-scale patterns have been used to  
44   argue for both an “expansionist” diversification paradigm<sup>1,3,4</sup>, and for constrained or  
45   diversity-dependent diversification<sup>2,7,9-11</sup>, resulting in great uncertainty.

46           We take a different approach to most previous studies by examining how species  
47 richness within tetrapod communities has changed through geological time. Assemblages  
48 from individual fossil localities represent communities of potentially-interacting species<sup>12</sup>,  
49 and long-term patterns of change in richness within these communities (=local richness or  
50 alpha diversity) provide a strong test of the processes that might regulate diversification at  
51 macro-scales<sup>8,12,13</sup>. Early work by Bambach<sup>12</sup> recognised that comparisons of within-  
52 community richness offer a way to at least partially circumvent many of the sampling biases  
53 that confound regional and global diversity curves derived from fossil data<sup>7,10</sup>. Our analysis  
54 specifically asks how the richness of tetrapod communities has changed through geological  
55 time. Patterns of local richness are related to global and regional patterns through spatial  
56 turnover and nestedness (beta diversity and provinciality)<sup>12,14</sup>. Addressing how richness has  
57 changed at these larger scales requires different forms of analysis (e.g. <sup>15,16</sup>) that are not  
58 utilised here. Nevertheless, our findings regarding local richness are relevant to debates about  
59 the processes that could stabilise diversification, either by limiting increases to species counts  
60 in local communities<sup>6,8,14</sup>, or by allowing them to remain high in spite of decreasing global  
61 richness<sup>17,18</sup>.

62           The expansionist model represents unconstrained diversification. It predicts  
63 continuous, and typically also large<sup>3</sup>, increases in local richness over geologically long  
64 intervals, spanning tens of millions of years. Within this paradigm, mass extinctions result in  
65 temporary setbacks to an otherwise upward diversity trajectory (e.g. <sup>3</sup>). In contrast,  
66 constrained models of diversification predict high rates of origination (speciation plus  
67 immigration) whenever lineages can exploit unoccupied ecospace. These abrupt increases in  
68 local richness are followed by extended intervals of relative stasis, as origination and  
69 extinction rates equilibrate to zero net diversification with increasing diversity<sup>19</sup>. Such  
70 slowdowns could be caused by negative biotic interactions within communities, such as

71 competition for finite resources<sup>14</sup>. Equilibria may also be reset episodically by ecological  
72 disruptions such as mass extinctions, major environmental changes, or the evolution of key  
73 innovations<sup>8,20</sup>. Patterns of local richness consistent with constrained diversification have  
74 been documented for several fossil groups<sup>21,22</sup>. However, local richness in fossil tetrapods is  
75 remarkably understudied and prior work is limited in its taxonomic, temporal and/or  
76 geographic scope<sup>2,7,23,24</sup>.

77         We document patterns of local richness in non-flying, non-marine (=terrestrial)  
78 tetrapods through their entire Phanerozoic history. We also dissect patterns for key subtaxa,  
79 including non-avian dinosaurs, mammals and squamates. Flying tetrapods were analyzed  
80 separately, because their fragile skeletons result in a much more unevenly sampled fossil  
81 record<sup>25</sup>. Our data, drawn from the Paleobiology Database<sup>26</sup>, comprise 145,332 taxon  
82 occurrences from 27,531 collections. We estimate local richness by counting species and  
83 genera per collection, including those specifically-indeterminate occurrences that must  
84 represent distinct species, because they record the presence of a higher taxon that is otherwise  
85 unknown in the collection (see Methods). Counts of taxa per collection are a widely-accepted  
86 proxy for local richness in the fossil record<sup>12</sup>. We also present counts of taxa per geological  
87 formation, which broadly corresponds to landscape-scale richness<sup>23</sup>.

88         We use two main forms of analysis to test hypotheses about the processes governing  
89 change in local richness through geological time: 1) linear model comparisons representing  
90 phases of “expansionist” and “constrained” diversification, using information only from  
91 exceptional localities that were parsed according to a set of objective, numerical criteria; and  
92 2) simulated null distributions based on resampling (with replacement) of empirical counts of  
93 species from the full set of localities, pooled according to time intervals. Both suggest a  
94 similar pattern comprising extended phases of stasis lasting tens of millions of years,  
95 interrupted by geologically-abrupt phase-shifts bringing about large increases in richness.



## 96     **Results and discussion**

97             Visual appraisal suggests that tetrapod local richness (counts of species per collection)  
98     experienced long periods of stability during the Permian–Triassic and from either the latest  
99     Cretaceous or earliest Cenozoic to the Recent, interrupted by an abrupt increase (in  
100     geological terms—spanning hundreds of thousands to, at most, a few million years; Fig. 1a).  
101     Total increases in local species richness were small compared to those implied by previous  
102     expansionist interpretations (entailing order-of-magnitude increases over the last 100 million  
103     years<sup>1,3</sup>)—compared to the richest Palaeozoic localities, local species richness had increased  
104     at most two-fold by the mid-Mesozoic, and at most three-fold by the latest Cretaceous–early  
105     Cenozoic. Following an initial slow increase in the early to mid-Carboniferous, observed  
106     local species richness rose steeply in the late Carboniferous (~25 species). Levels in the  
107     Permian did not greatly exceed those of the late Carboniferous (~30 species) and remained  
108     similar during the Late Triassic, 100 million years later, despite considerably more intense  
109     sampling. Patterns of local genus richness are similar (Supplementary Fig. 1), whereas  
110     landscape-scale richness (counts of species and genera per formation; Supplementary Fig. 2)  
111     suggest a more prolonged initial rise, lasting until the end of the Permian. The observed  
112     richness of exceptional collections (species and genera) increased by up to ~2.5 times  
113     between the end of the Triassic and the latest Cretaceous. Levels of local richness exceeding  
114     those from all earlier intervals occur in the Kimmeridgian–Tithonian stages of the Late  
115     Jurassic (~55 species; approximately double that of the Permian–Triassic), and in the  
116     Maastrichtian stage of the latest Cretaceous (~70–80 species; around 1.5 times that of the  
117     Late Jurassic). High observed local richness in the Kimmeridgian–Tithonian and  
118     Maastrichtian is driven by exceptional sampling of small-bodied taxa (mammals, squamates,  
119     turtles and lissamphibians). However, per-formation richness of non-flying terrestrial  
120     tetrapods at all taxonomic levels suggests little if any Mesozoic increase until the Campanian

(with the exception of the geographically-vast Morrison Formation, Late Jurassic, USA; Supplementary Fig. 2).

Simulated null distributions suggest that much (but not all) of the apparent variation in maximal local richness among intervals results from variation in sampling intensity. These support an interpretation of stasis in local richness interrupted by a single phase-shift following the end-Cretaceous extinction. Empirical patterns are substantially different to those obtained if richness per collection is randomly sampled from a single Phanerozoic-long pool. However, they deviate little from those obtained by random sampling from two pooled distributions divided by the Cretaceous/Palaeogene (K/Pg) boundary: one representing the Carboniferous–Cretaceous and the other representing the Cenozoic (Figs 2 and 3; Supplementary Figs 3 and 4; see Supplementary Information for full description of simulated null distributions). Adding an additional underlying pool to partition the data by geological era only marginally improves the fit over the two-phase pre-/post-K/Pg model, and is therefore not justified (Fig. 3). Although local richness clearly must have increased during the initial Palaeozoic radiation of terrestrial tetrapods, sampling is too limited to confidently resolve early changes in richness through comparison with the simulated null distributions (confidence intervals for the null are very large).

The weight of evidence supports a substantial increase in local richness across the K/Pg, followed by relative stasis toward the present (Fig. 1). A pattern of stasis in local richness before and after the K/Pg, broken by an abrupt two- to three-fold increase, is supported by both rarefaction curves of terrestrial tetrapod local richness quantiles for period-level bins (the Cretaceous is similar in richness to the Jurassic and Triassic but lower than the Paleogene, Neogene or Quaternary; Fig. 4; Supplementary Fig. 5), and comparisons between empirical curves of local richness quantiles and simulated null distributions (Figs 2 and 3). This is consistent with patterns of continent-scale sampling-standardized species richness<sup>10</sup>

and counts of species per formation. This interpretation might appear to be contradicted by the fact that the two richest Maastrichtian localities (Bushy Tailed Blowout and Lull 2 Quarry from the Lance Formation, USA) have species counts comparable to the richest Cenozoic localities. However, the K/Pg boundary has been subject to extraordinarily intense study, which could dramatically inflate the maximum observed estimates of local richness relative to earlier time intervals. These two localities are also substantially richer than all other Maastrichtian sites. On balance, we consider it more likely that tetrapod local richness increased immediately after the K/Pg boundary, rather than just before it.

Linear model comparisons likewise favour constrained models. The “species ~ phase” model explains richness of exceptional localities using only one covariate, describing the existence of distinct phases (see Methods) that are characterised by different average levels of local richness, and otherwise implies no continuous change in richness through time. This model is favoured for five of the nine numerically-defined sets of exceptional localities (median Akaike weight of 0.68, ranging from 0.051–0.74; median adjusted R-squared of 0.679, ranging from 0.511–0.766), although the “species ~ time + phase” model is sometimes favoured when lower richness quantile thresholds are used (“species ~ time + phase”; median Akaike weight of 0.276, ranging from 0.232–0.712; median adjusted R-squared of 0.679, ranging from 0.519–0.762; Supplementary Fig. 6; Supplementary Table 1). Models where time is the only explanatory variable, representing the expansionist paradigm, receive negligible support (median Akaike weight near zero). Furthermore, interval-specific regressions of richnesses of exceptional localities against time are non-significant, with near-zero slopes, for the late Carboniferous–Triassic (spanning ~160 million years) and Cenozoic (66 million years; see Supplementary Information).

Major groups of tetrapods also individually show early or stepwise increases, followed by extended periods of stasis. Observed local richness of non-avian dinosaurs

within exceptional localities rose steadily from the Late Triassic, reaching an apparent maximum in the Late Jurassic, followed by a slightly lower peak in the Campanian–Maastrichtian (Fig. 5a). Rarefaction curves of richness quantiles show that although non-avian dinosaur local richness was clearly lower in the Triassic than in the later Mesozoic, confidence intervals for the Jurassic and Cretaceous strongly overlap (Fig. 6a). Apparent peaks in Mesozoic mammals mirror those for dinosaurs (Fig. 5b), and confidence intervals for richness-quantile rarefaction curves also strongly overlap between the Jurassic and Cretaceous (Fig. 6b). Therefore, the maximum observed levels of local richness for two ecologically-important groups of large- and small-bodied tetrapods did not increase during an interval of nearly 100 million years between the Late Jurassic and end-Cretaceous. However, mammalian local richness increased abruptly by two- to three-fold across the K/Pg boundary (consistent with past studies documenting an extremely rapid recovery after the end-Cretaceous mass extinction<sup>27,28</sup>), reaching a second equilibrium that was maintained throughout the Cenozoic. It is plausible that the magnitude of apparent increase across the K/Pg could be exaggerated by the greater diagnosability of mammal teeth, but the contribution of this effect, if any, is unknown at present (see Methods). Magnitudes of local richness for Cenozoic mammals (60–70 species per collection or 100–200 species per formation) overlap with those obtained for surveys of present-day local faunas in Kenya (60–107 species for landscape-scale survey sites (120–1510 km<sup>2</sup> in area)<sup>29</sup>. Squamate local richness changed little from their first appearance in the Middle Jurassic until the Santonian, but nearly doubled in the Campanian–Maastrichtian, reaching levels that were sustained through most of the Cenozoic (Fig. 5d; Fig. 6c). Further investigation is needed to determine why the recovery of tetrapod communities after the end-Cretaceous mass extinction involved a rapid rebound to higher diversity equilibrium, while that following the end-Permian mass extinction did not.

196           Importantly, major taphonomic and collector biases show long-term trends of increase  
197 (Figs 1, b and c, and Supplementary Fig. 7), reflecting the widely-recognized tendency for  
198 geological sampling to improve towards the present<sup>30,31</sup>. Improved sampling towards the  
199 present systematically increases the chance of discovering highly diverse localities in  
200 younger deposits: better-sampled intervals tend to yield higher local richness estimates (as  
201 demonstrated by our simulated null distributions, richness-quantile rarefaction curves, and  
202 analyses of correlations between sampling proxies and local richness estimates; see Methods  
203 and Supplementary Information; Supplementary Figs 8 and 9). This makes our finding of  
204 statistical support for predominantly equilibrial patterns in uncorrected richness data  
205 particularly conservative. Correcting for poorer sampling within older deposits using  
206 comprehensive abundance data would most likely diminish the observed trend of increasing  
207 local richness through time.

208           The static patterns of local richness we document imply persistent constraints on  
209 increases in species counts within communities. Nevertheless, this does not necessarily  
210 indicate constraints at regional or global-scale richness, because patterns of richness at  
211 different spatial scales may become decoupled via changes in beta diversity or faunal  
212 provinciality<sup>14</sup>. Therefore, our results do not entirely preclude a postulated ten-fold expansion  
213 in global species richness over the last 100 million years<sup>32</sup>. However, they do demand  
214 substantial, and as-yet undocumented, increases in beta diversity (geographic turnover of  
215 community composition, or faunal provinciality) to accommodate such a profound increase if  
216 it occurred, and this scenario is strongly contradicted by regional-scale studies of sampling-  
217 standardised diversity patterns in Mesozoic–Cenozoic terrestrial tetrapods [e.g.<sup>2,7,10</sup>].

218           Ecologists increasingly regard modern communities as unsaturated<sup>6,33</sup>. A common  
219 interpretation of this hypothesis is that local and regional richness should rise in an  
220 essentially continuous fashion through palaeontological time<sup>3,6</sup>. This prediction is

inconsistent with a growing portfolio of evidence from the fossil record<sup>7,20,21,23</sup>. We find little support for the expansionist model of diversification within terrestrial tetrapods at the local scale. Instead, local richness shows constrained or asymptotic patterns over hundreds of millions of years, punctuated by rare but abrupt increases during the rise of major groups and following mass extinctions. Importantly, the effects of mass extinctions are very short-lived, with diversity rapidly rebounding to equal or surpass pre-extinction levels.

Whether or not communities are ever truly ‘saturated’, origination and extinction rates in local assemblages are essentially balanced on timescales of tens of millions of years, leading to equilibrial or constrained diversity patterns. Process-based explanations of this observation are not well-understood<sup>8</sup>, and many of the lines of evidence from ecological studies used to support unconstrained diversity dynamics might be compromised if present-day community structures are anomalous for the Phanerozoic due to human impacts<sup>34</sup>. However, our results do not demand that specific kinds of biotic interactions are responsible for observed patterns<sup>35</sup>, or even that communities are in equilibrium<sup>36,37</sup>. Reconciling patterns in the fossil record with ecological theory based on modern communities remains a major challenge in evolutionary biology, and one that can only be addressed by integrative studies that unite observations across a wide range of spatiotemporal scales.

## Methods

**Data download and processing.** We downloaded occurrence data for Tetrapodomorpha from the Paleobiology Database<sup>26</sup> (PaleoDB; <http://www.paleobiodb.org>) on 13 December 2017. The dataset comprises 157,847 taxon occurrences from 33,346 collections (= localities or local faunas) prior to removal of unsuitable data, and 145,332 taxon occurrences from 27,531 collections after cleaning.

We removed occurrences pertaining to marine tetrapods, traces, egg taxa [using lists of names modified from Benson et al. <sup>7</sup>], common wastebasket taxa (e.g. “*Crocodylus*”, “*Crocodylus*”, “*Alligator*” and “*Lacerta*”), and other dubious occurrences (e.g. non-avian dinosaurs in Cenozoic horizons). Any remaining Cenozoic marine tetrapod occurrences were excluded using sets of occurrence numbers contained within PaleoDB occurrence data downloads for marine mammal clades (Cetacea, Pinnipedimorpha and Sirenia; we did not remove any transitional forms that may lie outside these groups). Marine birds and snakes were not excluded, but make up relatively few occurrences. Occurrences for which preservation mode was listed as “trace”, “cast,trace” or “mold/impression,trace” were also removed. Collections with soft-tissue preservation (e.g. Lagerstätten deposits) were retained. Obvious “wastebasket” collections that formed distinct outliers (shown on Supplementary Fig.10; e.g. PaleoDB collection no. 13779, a collection from the Eocene locality of Gran Barranca, Argentina, that was created to house historical specimens not clearly linked in the literature to specific fossil sites) were excluded.

We removed collections with the largest geographic scale of “basin” or the largest stratigraphic scale of “group”. This is because changes in the scope of the geographic and temporal sampling universes may bias estimates of local richness. An idealized PaleoDB fossil collection represents an assemblage of fossils originating from a single stratigraphic horizon (i.e., a single bed, or group of beds) within a small geographic area (e.g. a quarry). However, due to differential reporting of stratigraphic and geographic data in the literature, collections may in practice represent geographic scales ranging from single hand-samples, to single outcrops, groups of outcrops, local (such as a series of outcrops occurring over several kilometers), and even basinal (e.g. fossils reported from coming from a particular stratigraphic unit, but without any detailed locality information provided) areas, and stratigraphic scales ranging from a single bed or group of beds to member, formation or

group-level scales. We retained “formation”-level collections, because PaleoDB enterers sometimes assign “formation” level stratigraphic scale even though the collection in question in fact occupies a single bed, simply because more precise stratigraphic information is not given in the literature.

To analyze individual clades, we taxonomically filtered the tetrapod occurrence dataset using occurrence ID numbers contained within separate PaleoDB data downloads for non-avian dinosaurs (Dinosauria excluding Aves), birds (Aves), non-flying mammals (Mammaliaformes excluding Chiroptera), bats (Chiroptera), squamates (Squamata), turtles (Testudinata), and crocodylians and their stem-group (Pseudosuchia).

**Time bins.** Composite time bins of approximately equal length were used to calculate simulated null distributions, trends in sampling biases and correlations between sampling variables (see below). This binning scheme was based on that used by Benson et al.<sup>7</sup>, which was in turn modified from the scheme used by the original Paleobiology Database portal (now Fossilworks; <http://www.fossilworks.org>). On average, these “equal-length” bins are ~9 myr in duration, but range from 19.5 myr for Tr4 (Norian) to 1.806 for Ng4 (Calabrian, Middle Pleistocene, Late Pleistocene and Holocene). Definitions of equal-length bins are given in Supplementary Table 2. Data were binned by midpoint ages of collections or formations.

**Estimating local richness.** Fossil localities comprise assemblages of potentially interacting species but, in contrast to instantaneous snapshots from present-day communities, assemblages are generally time-averaged on scales of tens to hundreds of millennia. Measurements of local richness over palaeontological timescales are important because they smooth out short-term fluctuations due to nonequilibrium processes<sup>8</sup> that may obscure longer-term patterns.



We estimate local richness using simple face-value counts of taxa present within localities because sampling-standardised estimates of richness within collections require abundance data, which are not systematically available. Nevertheless, our use of face-value counts allows direct comparison with older studies that used face-value global richness counts to argue for expansionist diversification<sup>1,3</sup>. All of our counts of species include specifically-determinate occurrences plus “indeterminates” — occurrences that are not resolved to species level, but nevertheless indicate the presence of a distinct species in that collection. For example, an occurrence of “Muridae indet.” would be counted only if there were no occurrences of murids resolved to finer taxonomic levels within the collection. This measure provides the most accurate estimate of species-level richness, because it tallies every distinct species recognized in a collection regardless of whether or not it has been identified to species level.

To determine whether specifically-indeterminate occurrences represented distinct species, we used the hierarchy of taxonomic names in the PaleoDB. This was achieved by: 1) determining all of the unique accepted names represented by occurrences within a collection; 2) obtaining all of the names in the taxonomic hierarchy above each of these accepted names; and 3) finding which accepted names were not present in the pooled list of unique names drawn from the taxonomic hierarchies. Informal species identified within a collection (such as “Chiroptera informal indet. sp. 1”) were counted as separate species. For full operational details, see our R function ‘countLocalRichness’ in the supplementary analysis files. Counts of genus richness likewise include generically-indeterminate occurrences that must represent distinct genera, using the same procedure outlined above (although without tallying “informal indet.” species).

Patterns of local richness were visualized by plotting counts of taxa per collection or formation against their midpoint ages. Although we focus on “global” patterns from

aggregated global data, we also plotted regional patterns of local richness for five continents (North America, South America, Europe, Africa and Asia; note that Russia was assigned to Asia). Patterns of local richness were also dissected by palaeolatitudinal zone (low = 0°–30°, mid = 30°–60°, and high = 60°–90° palaeolatitude).

**Defining exceptional localities using objective numerical criteria.** Unlike extant ecosystems, fossil samples—especially for terrestrial tetrapods—are characterised by strongly negatively-skewed distributions of richness per collection. This occurs because of a pervasive issue of sample incompleteness: most localities only record a tiny fraction of the original biota, and are thus largely uninformative about patterns of local richness. We therefore focus our qualitative interpretations of the data, and our quantitative linear model comparisons, on exceptional, extensively-sampled localities. These record the most complete snapshots of ancient ecosystems, although they are relatively few in number (Fig. 1a, Supplementary Figs 6 and 11; key information about a selected set of exceptional localities is given in Supplementary Table 3).

We identify these using objective numerical criteria based upon co-occurrences of higher taxa (e.g., including both small-bodied groups such as mammals, and large-bodied groups such as dinosaurs) and richness quantiles. Richness quantiles were calculated within period-level bins. We explored parameter space using nine objective sets of exceptional localities, created by combining three quantile thresholds for non-flying terrestrial tetrapod species richness (0.99, 0.995 and 0.998) and three levels of taxonomic co-occurrence criteria (“None” = no restrictions; “Moderate” = localities containing at least one mammal, one dinosaur and one squamate during their ranges; and “Stringent” = at least one mammal, one dinosaur, one squamate, one turtle, and either a pseudosuchian, lissamphibian or flying tetrapod). These taxonomic co-occurrence criteria ensure that both large- and small-bodied taxa are present. Because most of these major groups did not arise until later in the Mesozoic,

prior to 200 Ma localities could be defined as exceptional only if they contained at least 20 species (“Moderate” and “Stringent” levels of taxonomic co-occurrence criteria only).

**Quantitative analyses of local richness.** To test alternative hypotheses about modes of diversification (e.g., evaluating the relative support for continuous/gradual/exponential increases through time versus periods of stasis broken by sudden changes in diversity equilibria), we fitted a range of linear models to values of non-flying terrestrial tetrapod local richness within exceptional localities. These linear models represent either: 1) continual increases in richness through time (expansionist models), or 2) stepwise increases separated by extending intervals of approximate stasis, during which short-term variability does not accumulate into longer-term increases (constrained models).

We also document trends in key biases that influence the preservation and recovery potential of fossils, and therefore inform our interpretations. We document substantial increases through the latest Cretaceous and Cenozoic in: 1) the number of fossil collections and their geographic spread; 2) the frequency and number of bulk-sampled collections; 3) collections derived from unlithified or poorly-lithified sediments; 4) collections from low paleolatitudes (Supplementary Fig. 7); and 5) collections from depositional environments that do not preserve well in deep time (see discussion below; Supplementary Fig. 7c). All of these lines of evidence indicate that younger deposits either favor the preservation of rich faunas or allow easier extraction and diagnosis of fossil specimens. This progressively expands the size of the accessible taxonomic sampling universe, driving increases in within-collection sample completeness, and elevating raw estimates of local richness nearer the present.

We controlled for sampling-intensity biases on inferred patterns of local richness using three approaches: by simulating null distributions of local richness quantiles; generating rarefaction curves of per-bin local richness; and analysing correlations between sampling proxies and per-bin local richness estimates. Together, these analyses suggest that:

1) support for our interpretation is substantially strengthened by controlling for variation in sampling intensity through time; 2) our interpretation is robust to the use of different subsets of the data; and 3) variation in factors such as environments are relatively unimportant for the types of analyses done here, having only small effects on inferred patterns.

*Testing diversification hypotheses.* We used the Akaike Information Criterion with small-sample-size correction (AICc) to evaluate the relative fit of an intercept-only null model (using the formula “species ~ 1”) of static non-flying terrestrial tetrapod richness against a simple linear model of richness as a function of time, plus multiple regressions incorporating time and/or a “diversification phase” factor as a covariate or interaction term<sup>38,39</sup>. The phase model uses two covariates: time, and a categorical variable consisting of temporal intervals corresponding to diversification phases (phase1 = Devonian–Mississippian, phase 2 = Pennsylvanian–Triassic, phase 3 = Jurassic–Cretaceous [beginning in the Tr4 time bin for regressions on individual phases, because the Early Jurassic lacks exceptional localities] and phase 4 = Maastrichtian–Cenozoic), allowing the intercept to vary through time while sharing the same slope. No exceptional localities are known from Phase 1. Additionally, we fitted individual regressions to the diversification phases defined above. We did not attempt to fit a multiphase logistic model because the temporal resolution of the data is too coarse and the density of data points too low in many key intervals, particularly in the early Carboniferous and Early to Middle Jurassic.

*Sampling intensity biases.* Opportunities for sampling terrestrial localities increase dramatically nearer the present, driven by the increasing availability of fossil-bearing sediments from the Late Cretaceous onwards: over half of all the exposed rocks from terrestrial environments date from the Cretaceous and Miocene<sup>30</sup>. There are substantial increases in per-bin counts of collections and occupied equal-area grid cells (a measure of palaeogeographic spread; Fig. 1c [variables log-transformed] and Supplementary Fig. 7 [un-

transformed variables]), especially from low palaeolatitudes, which are poorly known during earlier intervals.

Unlike global or regional richness, increased sampling of localities or geographic regions does not directly or mechanistically cause local richness to increase. Estimates of local richness are not additive with respect to sampling of new localities—rather, they are drawn probabilistically from an underlying distribution. The process is analogous to playing a slot machine: a single attempt may yield a spectacular win, while many attempts may fail to net a return. All else being equal, however, playing more frequently (i.e., sampling the fossil record more intensively) increases one's chances of winning. As a result, it is important to analytically control for sampling intensity when documenting local richness patterns; we do this using simulated null distributions, rarefaction curves of local richness quantiles and correlation tests.

Simulated null distributions. Our simulated null distributions make use of a different principle to the linear models. Instead of focusing only on exceptional localities, they simulated how variation in counts of localities through time could bias curves of per-bin richness quantiles when values of richness per collection are drawn probabilistically from a fixed underlying distribution. This distribution is simply the full set of per-collection richness values, and is either 1) lumped to a single, Phanerozoic-long pool, or 2) split into larger numbers of smaller pools delimited by time, and represent hypotheses about phase-shifts in local richness equilibria.

The simulations comprised 1000 independent trials. In each trial, the richness value for each collection in the full Phanerozoic dataset was drawn at random, with replacement, from a pooled set of local richness values. Four pools were used: a single Phanerozoic pool; pre- and post-K/Pg pools, era pools (Pz, Mz and Cz), and diversification-phase pools (with boundaries at the T/J and K/Pg boundaries). Simulations using multiple pools represent

hypotheses about shifts in local richness. Richness quantiles were then calculated for each equal-length bin (0.5, 0.75, 0.9, 0.95, 0.99 and 1 [1 = the per-bin maximum]). Mean values for per-bin richness quantiles were then calculated across all trials, along with 95% CIs. Confidence intervals for the empirical curves were calculated using 999 bootstrap replicates. Both null and empirical curves were smoothed using loess regression to de-emphasise bin-to-bin noise, but the null distributions use a slightly higher 'span' to increase smoothing (0.25 vs 0.1 for the empirical curve).

Rarefaction curves of local richness quantiles. We also used subsampling to generate rarefaction curves for geological periods, allowing per-bin quantiles of local richness for terrestrial tetrapods and major subgroups to be compared at different levels of comparable sampling intensity. We calculated rarefaction curves of local richness quantiles (at quantile levels ranging from 0.9–1), rarefied by collection, within period-length bins. Richness quantiles below 0.9 were found to be uninformative, as they were too heavily leveraged by abundant but highly depauperate localities. These curves reveal the expected local richness quantile values across repeated draws of a fixed number of collections, thus controlling for the number of sampling opportunities.

Correlation analyses. Lastly, correlation analyses show how per-bin changes in local richness relate to sampling intensity on long and short timescales. It is important to assess the short-term correlation between local richness and sampling proxies, because this allows us to evaluate the degree to which sampling effort directly controls within-collection richness. To determine the relative influence of short- and long-term factors governing the relationship between local richness quantiles and sampling, as quantified by counts of collections and equal-area occupied grid-cells, we evaluated: 1) the correlation between raw variables using Spearman's rank-order correlation; and 2) the correlation between variables after detrending the data series using an ARIMA model. All variables were log-transformed.

The optimal degree of differencing and values for autoregressive and moving average components in ARIMA models for each data series were automatically chosen using the function `auto.arima` in the R package `forecast`<sup>40</sup>. If the correlation after detrending is substantially stronger than the raw correlation, then the relationship must be driven by long-term trends (such as a long-term increase in the intensity and distribution of sampling), rather than short-term fluctuations in sampling.

*Lithification biases.* It also becomes easier to find and extract fossils from younger deposits. A substantial rise in counts and proportions of unlithified or poorly-lithified terrestrial sediments, accompanied by similar increases in the use of bulk-sampling methods, begins in the Late Cretaceous (Fig. 1c, Supplementary Figs 7b and 12). Bulk-sampling of unlithified sediments permits more exhaustive sampling of a local fauna<sup>41</sup>. This should cause within-site sample completeness, and thus raw estimates of local richness, to increase systematically towards the present<sup>41,42</sup>. For example, the lithification bias might account for as much as half of the three- to four-fold increases in local richness of marine invertebrates during the Cenozoic<sup>43</sup>. Notably, there is a pronounced peak in counts of bulk-sampled localities during the Campanian–Maastrichtian that might account for the apparent end-Cretaceous rise in tetrapod local richness (Supplementary Fig. 7). The lithification bias can be partially addressed by applying sampling-standardization methods. However, the abundance data required are not generally available in the literature for Phanerozoic tetrapods.

*Environmental heterogeneity.* We cannot directly account for variation in the environments represented by exceptional localities through time but we can show that, with one important exception, there are not substantial systematic changes in these environments through the study interval (although there is usually considerable variation; see Supplementary Figs 13 and 14; see also Supplementary Table 3). The one exception results

from the large increases in geologically-ephemeral environments such as cave deposits within the past five to ten million years<sup>31</sup>, which we excluded from our analyses (Supplementary Fig. 7c). In the Plio–Pleistocene, lithification biases combine with the wide geographic distribution of depositional environments that are poorly represented in the deeper fossil record to markedly increase the quality of sampling at the local scale.

These environments, dubbed “doomed sediments” by Holland<sup>31</sup>, include cave-fill deposits, tar-pits and many fluvial and lacustrine environments not located in subsiding basins and which only rarely survive into the deep-time rock record because they are more frequently erased by early erosion. Such environments are not definitively “doomed” over long timescales, but they are substantially more prevalent near the present than in deep time. The progressive loss of deposits from these depositional environments creates an increasing preservational discrepancy over time and systematically changes the rate of fossil preservation from shallow to deep time<sup>31</sup>. In particular, the large increase in Plio–Pleistocene cave-fill environments, which preserve groups that are rarely fossilized, such as birds, bats and lissamphibians<sup>44</sup>, drives a coincident spike in sampled local richness of flying tetrapods (Supplementary Fig. 15). We therefore omit Plio–Pleistocene karst environments from our main figures and analyses. However, ancient cave-systems pre-dating the Plio–Pleistocene (identified in the PaleoDB as general “karst” or “fissure-fill” environments) were retained. These karst deposits, especially fissure-fills and sink holes, provide us with rare but exceptional and important windows onto ancient faunas, such as the Triassic/Jurassic fissure fill deposits from the southwest UK and Richards Spur, from Permian deposits in the Midwest USA.

*Taphonomic biases.* Taphonomic factors causing differences in preservation potential among higher taxa may bias local richness of individual groups up or down. Nevertheless, this should not obscure relative changes through time, so long as these biases are consistent



through time. However, consistently high levels of non-flying terrestrial tetrapod local richness during the Cenozoic may be in part an artifact of the ecological ascendancy of crown-group mammals (including increases in richness and abundance). Durable mammal teeth are easily preserved and diagnosed from limited fossil material. This permits more consistently fair comparisons of richness through time, and results in higher apparent local richness than that of groups that were likely at least as diverse. For example, today, on a global level, squamates are more than twice as diverse as non-flying mammals, yet the apparent local richness of mammals is two- to three-fold greater over much of the Cenozoic (Fig. 5, b and c).

*Geographic biases.* Shifts in spatial sampling through deep time could potentially affect apparent patterns of local richness. Today, latitudinal climate variation is a key driver of richness, but sampling in our dataset is dominated by records from temperate palaeolatitudes (Supplementary Fig. 16). Patterns from well-sampled continents such as Europe and North America are comparable to those of the aggregated global data (Supplementary Fig.17). However, comparisons between the Palaeozoic and later intervals may be complicated because the record up until the mid-Permian is predominantly palaeoequatorial, whereas much of the later record derives from palaeotemperate regions. This bias could inflate Palaeozoic local richness relative to later time intervals.

To investigate the potential influence of preservational factors on patterns of tetrapod local richness, we visualized the distribution of collections representing poorly-lithified or unlithified sediments, those that had been bulk-sampled, and those originating from low palaeolatitudes (within 30° of latitude from the palaeoequator). There are particularly large Cenozoic increases in sampling at low palaeolatitudes<sup>45</sup> (Supplementary Fig. 7c). Large-scale terrestrial rock-record biases are also affected by the proximity to the modern equator, where outcrops are limited by greater vegetation cover<sup>46</sup>. Additionally, rapid decay of organic

material near the terrestrial palaeoequator reduces the chance of fossilization in the first place<sup>47</sup>, a bias which would work in opposition to recovering modern-style latitudinal diversity gradients in the fossil record.

**Life Sciences Reporting Summary.** Further information on experimental design is available in the Life Sciences Reporting Summary.

**Data and code availability.** The data used in this study were downloaded from the Paleobiology Database (<http://www.paleobiodb.org>) and have been archived, together with all custom analysis scripts, on Dryad (<https://doi.org/10.5061/dryad.3v0p84v>).

## References

1. Benton, M. J. Diversification and extinction in the history of life. *Science* **268**, 52–58 (1995).
2. Alroy, J. in *Speciation and Patterns of Diversity* (eds. Butlin, R., Bridle, J. & Schluter, D.) 301–323 (Cambridge University Press, 2009). doi:10.1017/CBO9780511815683.017
3. Benton, M. J. & Emerson, B. C. How did life become so diverse? The dynamics of diversification according to the fossil record and molecular phylogenetics. *Palaeontology* **50**, 23–40 (2007).
4. Kalmar, A. & Currie, D. J. The completeness of the continental fossil record and its impact on patterns of diversification. *Paleobiology* **36**, 51–60 (2010).
5. Vermeij, G. J. & Grosberg, R. K. The great divergence: when did diversity on land exceed that in the sea? *Integr. Comp. Biol.* **50**, 675–682 (2010).
6. Harmon, L. J. & Harrison, S. Species diversity is dynamic and unbounded at local and continental scales. *Am. Nat.* **185**, 584–593 (2015).
7. Benson, R. B. J. *et al.* Near-stasis in the long-term diversification of Mesozoic tetrapods. *PLoS Biol.* **14**, e1002359 (2016).
8. Rabosky, D. L. & Hurlbert, A. H. Species richness at continental scales is dominated by ecological limits. *Am. Nat.* **185**, 572–583 (2015).
9. Liow, L. H. & Finarelli, J. A. A dynamic global equilibrium in carnivoran diversification over 20 million years. *Proc. R. Soc. B* **281**, 20132312–20132312 (2014).

- 546 10. Close, R. A., Benson, R. B. J., Upchurch, P. & Butler, R. J. Controlling for the species-area effect  
547 supports constrained long-term Mesozoic terrestrial vertebrate diversification. *Nat. Commun.* **8**, 15381  
548 (2017).
- 549 11. Cantalapiedra, J. L., Domingo, M. S. & Domingo, L. Multi-scale interplays of biotic and abiotic drivers  
550 shape mammalian sub-continental diversity over millions of years. *Sci Rep* **8**, 1–8 (2018).
- 551 12. Bambach, R. K. Species richness in marine benthic habitats through the Phanerozoic. *Paleobiology*  
552 (1977).
- 553 13. Wiens, J. J. The causes of species richness patterns across space, time, and clades and the role of  
554 ‘ecological limits’. *Q. Rev. Biol.* **86**, 75–96 (2011).
- 555 14. Alroy, J. Limits to species richness in terrestrial communities. *Ecology* **53**, 1211–9 (2018).
- 556 15. Davis, E. B. Mammalian beta diversity in the Great Basin, western USA: palaeontological data suggest  
557 deep origin of modern macroecological structure. *Global Ecology and Biogeography* **14**, 479–490  
558 (2005).
- 559 16. Vavrek, M. J. & Larsson, H. C. E. Low beta diversity of Maastrichtian dinosaurs of North America.  
560 *PNAS* **107**, 8265–8268 (2010).
- 561 17. Primack, R. B. *et al.* Biodiversity gains? The debate on changes in local- vs global-scale species  
562 richness. *Biological Conservation* **219**, A1–A3 (2018).
- 563 18. Cardinale, B. J., Gonzalez, A., Allington, G. R. H. & Loreau, M. Is local biodiversity declining or not?  
564 A summary of the debate over analysis of species richness time trends. *Biological Conservation* **219**,  
565 175–183 (2018).
- 566 19. Sepkoski, J. J., Jr. A kinetic model of Phanerozoic taxonomic diversity. III. Post-Paleozoic families and  
567 mass extinctions. *Paleobiology* **10**, 246–267 (1984).
- 568 20. Alroy, J. Dynamics of origination and extinction in the marine fossil record. *PNAS* **105 Suppl 1**, 11536–  
569 11542 (2008).
- 570 21. Knoll, A. H. in (eds. Diamond, J. & Case, T. J.) 126–141 (Harper & Row, 1986).
- 571 22. Powell, M. G. & Kowalewski, M. Increase in evenness and sampled alpha diversity through the  
572 Phanerozoic: comparison of early Paleozoic and Cenozoic marine fossil assemblages. *Geology* **30**, 331  
573 (2002).
- 574 23. Stucky, R. K. in *Current Mammology* **2**, 375–432 (1990).

575 24. Barry, J. C. *et al.* Faunal and environmental change in the late Miocene Siwaliks of northern Pakistan.  
576 *Paleobiology* **28**, 1–71 (2002).

577 25. Brocklehurst, N., Upchurch, P., Mannion, P. D. & O'Connor, J. K. The completeness of the fossil record  
578 of Mesozoic birds: implications for early avian evolution. *PLoS ONE* **7**, e39056 (2012).

579 26. The Paleobiology Database.

580 27. Alroy, J. The Fossil Record of North American Mammals: Evidence for a Paleocene Evolutionary  
581 Radiation. *Syst. Biol.* **48**, 107–118 (1999).

582 28. Wilson, G. P. in *Through the End of the Cretaceous in the Type Locality of the Hell Creek Formation in*  
583 *Montana and Adjacent Areas* **503**, 365–392 (Geological Society of America, 2014).

584 29. Tóth, A. B., Lyons, S. K. & Behrensmeyer, A. K. A century of change in Kenya's mammal  
585 communities: increased richness and decreased uniqueness in six protected areas. *PLoS ONE* **9**, e93092  
586 (2014).

587 30. Wall, P. D., Ivany, L. C. & Wilkinson, B. H. Impact of outcrop area on estimates of Phanerozoic  
588 terrestrial biodiversity trends. *Geol. Soc. London Spec. Publ.* **358**, 53–62 (2011).

589 31. Holland, S. M. The non-uniformity of fossil preservation. *Philos. T. Roy. Soc. B.* **371**, 20150130 (2016).

590 32. Benton, M. J. Origins of Biodiversity. *PLoS Biol.* **14**, e2000724 (2016).

591 33. Mateo, R. G., Mokany, K. & Guisan, A. Biodiversity models: what if unsaturation is the rule? *Trends*  
592 *Ecol. Evol.* (2017). doi:10.1016/j.tree.2017.05.003

593 34. Lyons, S. K. *et al.* Holocene shifts in the assembly of plant and animal communities implicate human  
594 impacts. *Nature* **529**, 80–83 (2016).

595 35. Hubbell, S. P. *The Unified Neutral Theory of Biodiversity and Biogeography (MPB-32)*. (Princeton  
596 University Press, 2011).

597 36. Connell, J. H. Diversity in tropical rain forests and coral reefs. *Science* **199**, 1302–1310 (1978).

598 37. Huston, M. A general hypothesis of species diversity. *The American Naturalist* **113**, 81–101 (1979).

599 38. Benson, R. B. J. & Mannion, P. D. Multi-variate models are essential for understanding vertebrate  
600 diversification in deep time. *Biol. Lett.* **8**, 127–130 (2012).

601 39. Benson, R. B. J. & Upchurch, P. Diversity trends in the establishment of terrestrial vertebrate  
602 eco-systems: Interactions between spatial and temporal sampling biases. *Geology* **41**, G33543.1–46  
603 (2012).

40. Hyndman, R. J. & Khandakar, Y. Automatic time series forecasting: the forecast package for R. *J. Stat. Soft.* **27**, (2008).
41. Alroy, J. *et al.* Phanerozoic trends in the global diversity of marine invertebrates. *Science* **321**, 97–100 (2008).
42. Sessa, J. A., Patzkowsky, M. E. & Bralower, T. J. The impact of lithification on the diversity, size distribution, and recovery dynamics of marine invertebrate assemblages. *Geology* **37**, 115–118 (2009).
43. Hendy, A. J. W. The influence of lithification on Cenozoic marine biodiversity trends. *Paleobiology* **35**, 51–62 (2009).
44. Jass, C. N. & George, C. O. An assessment of the contribution of fossil cave deposits to the Quaternary paleontological record. *Quaternary International* **217**, 105–116 (2010).
45. Allison, P. A. & Briggs, D. E. G. Paleolatitudinal Sampling Bias, Phanerozoic Species-Diversity, and the End-Permian Extinction. *Geology* **21**, 65–68 (1993).
46. Noto, C. R. in *Taphonomy* (eds. Allison, P. A. & Bottjer, D. J.) **32**, 287–336 (Springer, 2010).
47. Behrensmeyer, A. K., Kidwell, S. M. & Gastaldo, R. A. Taphonomy and paleobiology. *Paleobiology* **26**, 103–147 (2000).

**Supplementary Information** is linked to the online version of the paper at <http://www.nature.com/nature>.

**Acknowledgements.** We thank all contributors to the Paleobiology Database. This research was funded by the European Union’s Horizon 2020 research and innovation programme 2014–2018 under grant agreement 637483 (ERC Starting Grant TERRA, RJB). PDM was supported by a Leverhulme Trust Early Career Fellowship (ECF-2014-662) and a Royal Society University Research Fellowship (UF160216).

**Author contributions.** RAC, RBBB and RBJ conceived the study. JA, AKB, JB, RBBB, RJB, MTC, TJC, ED, PDM and MU contributed to the dataset. RAC designed and conducted the analyses. RAC wrote the manuscript. RBBB, JA and MTC provided methodological advice. RJB and RBBB drafted portions of the manuscript. All authors provided critical comments on the manuscript.

**Competing interests.** The authors declare no competing interests.

**Author Information** Reprints and permissions information is available at [www.nature.com/reprints](http://www.nature.com/reprints). The authors declare no competing financial interests. Correspondence and requests for materials should be addressed to RAC ([r.a.close@bham.ac.uk](mailto:r.a.close@bham.ac.uk)).

## Figure Captions

**Fig. 1. Patterns of local richness for Phanerozoic terrestrial non-flying tetrapods and time series of key fossil-record sampling metrics.** **a**, local species richness (red points denote exceptional localities identified using moderately-strict taxonomic co-occurrence criteria and a richness quantile threshold of 0.995). **b**, Counts of occupied equal-area grid cells (50 km spacing), total counts of collections, counts of bulk-sampled and unlithified or poorly-lithified collections (note logarithmic scale). For age ranges of approximately equal-length bins used in panel b, see Methods.

**Fig. 2. Comparison between the empirical curve of local species richness (quantile = 0.9) for terrestrial tetrapods and simulated null distributions.** Richness quantiles calculated for equal-length bins. Underlying pools of local richness values for simulated null distributions were drawn either from the whole Phanerozoic, or separate pre-/post-K/Pg or era-level pools (median and 95% confidence intervals calculated from 1000 bootstrap replicates). The null distribution generated from a single Phanerozoic pool of local richness values fits the empirical richness curve poorly. Using separate pre-/post-K/Pg pools substantially improves the fit (see also Fig. 3), while adding a third pool (Era Pools) makes little additional difference. For additional richness quantile levels, see Supplementary Fig. 3.

**Fig. 3. Residual sums of squares for simulated null distributions of local richness (quantile = 0.9) using Phanerozoic, Pre-/Post-K/Pg and Era Pools.** Using separate pre-/post-K/Pg pools substantially improves the fit compared to a single Phanerozoic pool, while adding a third pool (Era Pools) makes only a negligible improvement. For additional richness quantile levels, see Supplementary Fig. 4.

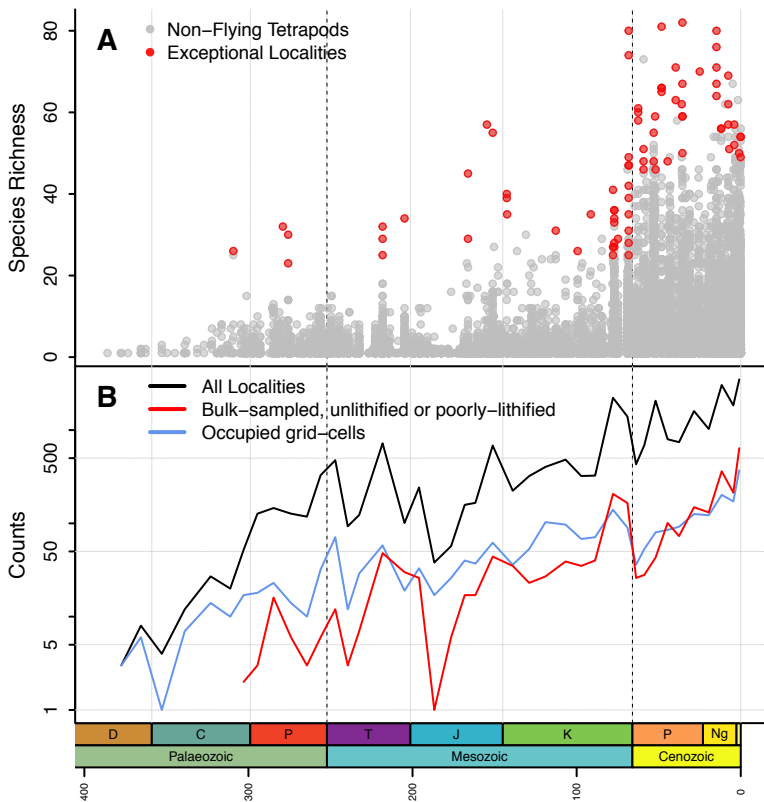
**Fig. 4. Rarefaction curves of local richness (quantile = 0.95) per period bin for terrestrial tetrapods.** Shaded regions show 95% confidence intervals calculated by

666 bootstrapping (1000 replicates). **a**, Cenozoic. **b**, Mesozoic. **c**, Palaeozoic. Abbreviations: Q =  
667 Quaternary, Ng = Neogene, Pg = Palaeogene, K = Cretaceous, J = Jurassic, T = Triassic, P =  
668 Permian, C = Carboniferous, D = Devonian.

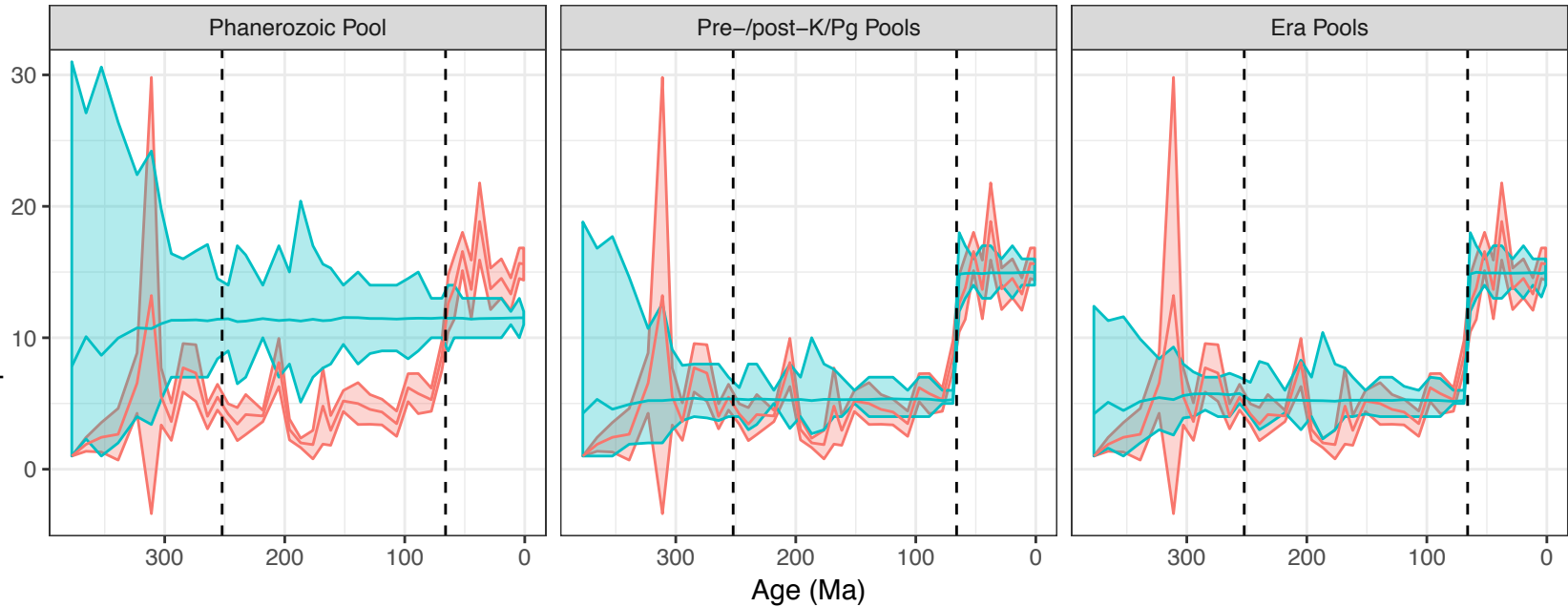
669 **Fig. 5. Clade-level patterns of local species richness. a**, non-avian dinosaurs. **b**, non-  
670 chiropteran mammaliamorphs. **c**, squamates.

671 **Fig. 6. Rarefaction curves of local richness (quantile = 0.95) per period bin for major**  
672 **tetrapod subclades (non-avian dinosaurs, non-chiropteran mammaliamorphs and**  
673 **squamates).** Shaded regions show 95% confidence intervals calculated by bootstrapping  
674 (1000 replicates). Abbreviations: Q = Quaternary, Ng = Neogene, Pg = Palaeogene, K =  
675 Cretaceous, J = Jurassic, T = Triassic, P = Permian, C = Carboniferous, D = Devonian.

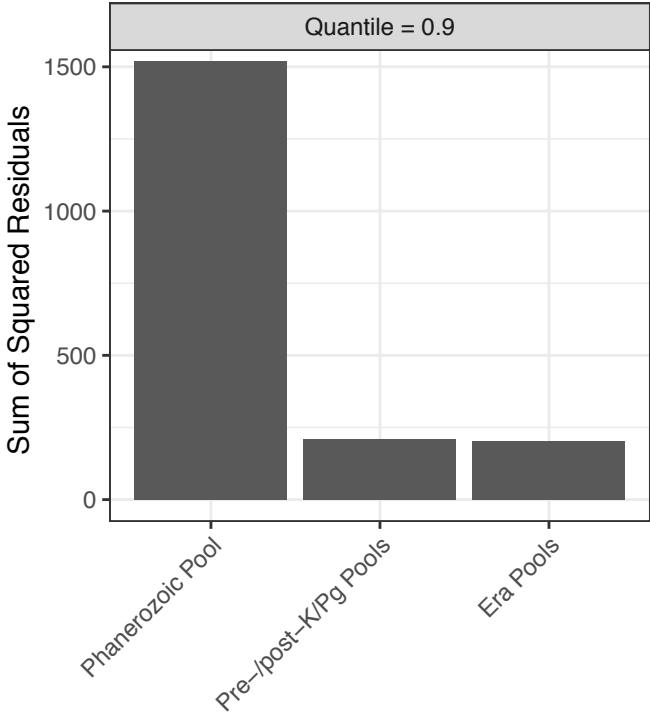


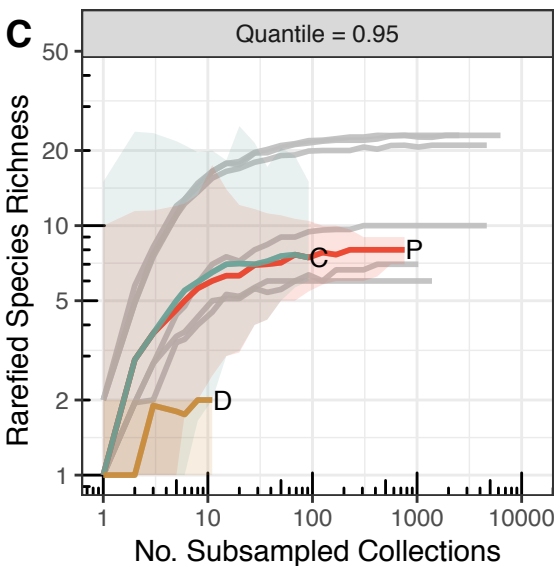
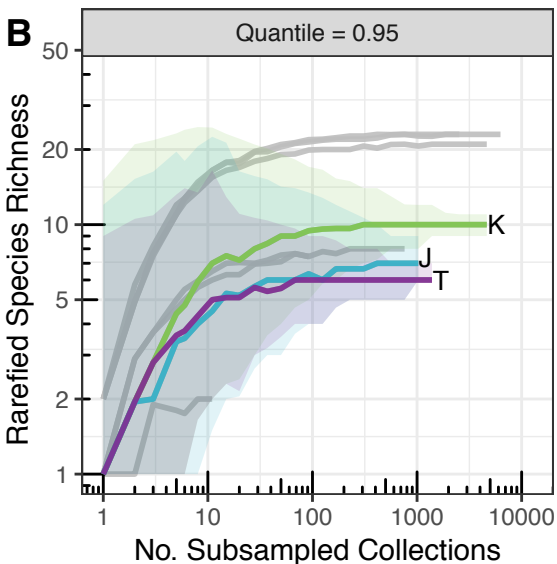
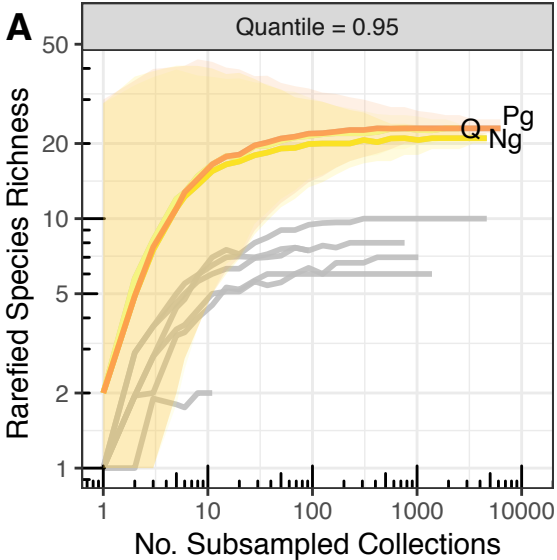


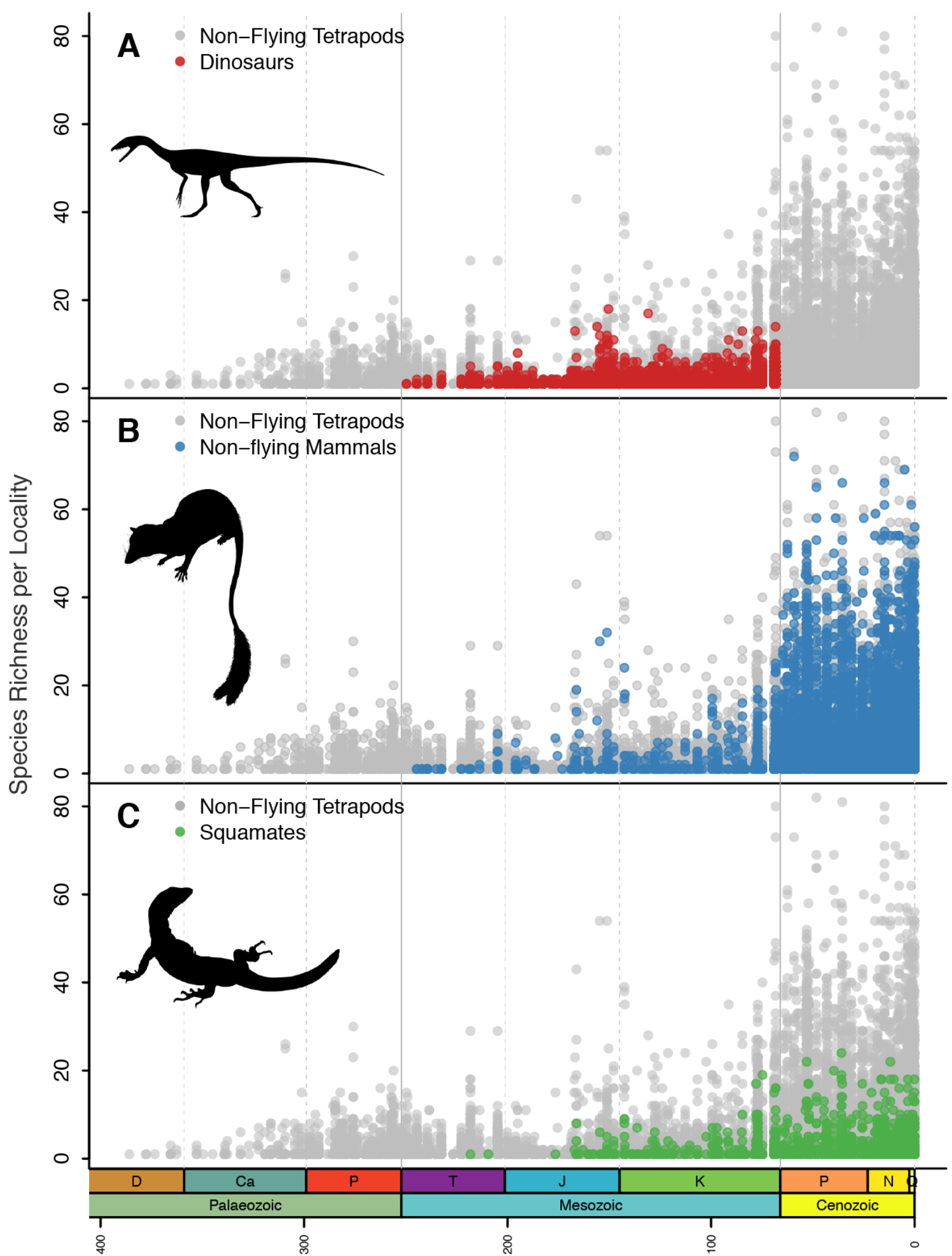
Non-flying Tetrapod  
Species Richness



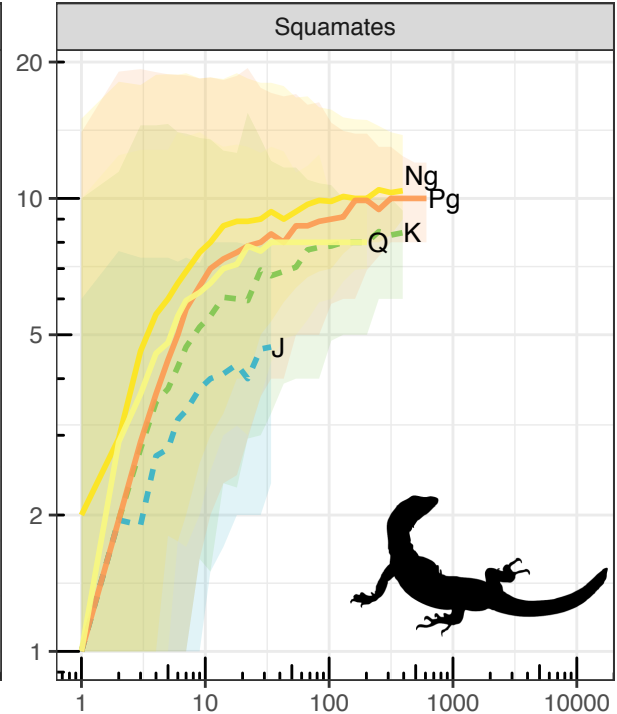
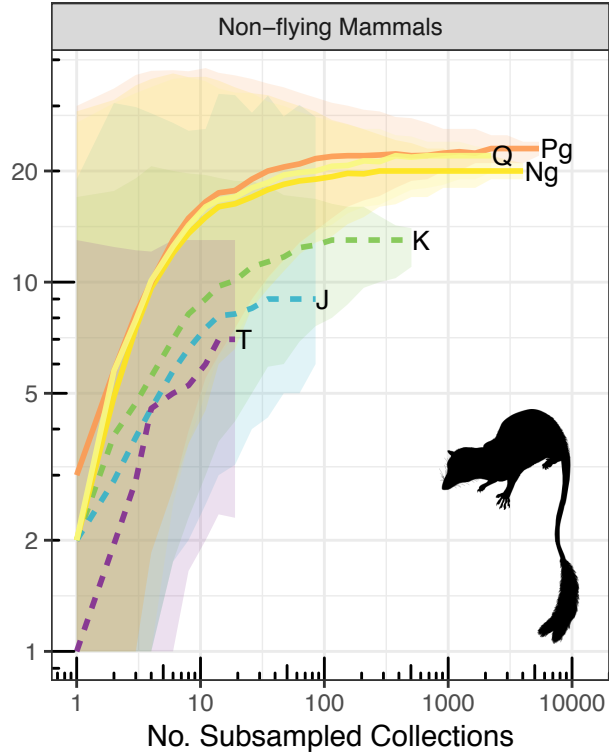
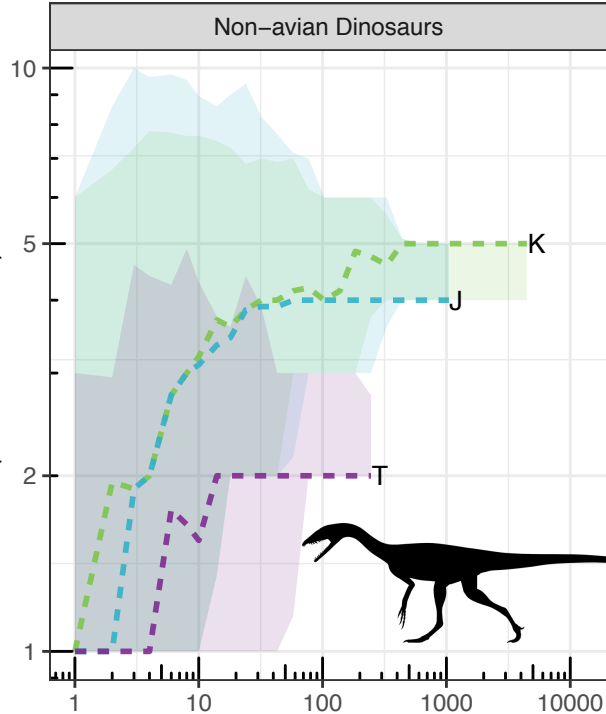
Dataset empirical null







Rarefied Local Species Richness  
(Quantile = 0.95)



# Supplementary Information

## Supplementary Results

### Linear models of non-flying tetrapod local richness

Across the nine numerically-defined sets of superlocalities, all models apart from the intercept-only were statistically significant (Supplementary Fig. 6; Supplementary Table 1). Akaike weights indicate strongest support for the “species ~ phase” model (median Akaike weight of 0.68, ranging from 0.051–0.74; median adjusted R-squared of 0.679, ranging from 0.511–0.766), with this being the preferred model in five of the nine superlocality sets (especially when using higher richness quantile thresholds). However, there is also some support for the model in which time is a covariate (“species ~ time + phase”; median Akaike weight of 0.276, ranging from 0.232–0.712; median adjusted R-squared of 0.679, ranging from 0.519–0.762). This was the preferred model for the remaining four superlocality sets, especially when using lower richness quantiles to define superlocality sets (using lower richness quantiles may capture localities that are less clearly exceptional). In cases where the favored model was “species ~ time + phase”, the coefficient of time was significant with slope of nearly zero ( $\sim -0.001$ ).

The intercept-only model and models including time and phase with an interaction term or time alone received little support. This indicates that there is little evidence for substantial increases in local richness within phases, but that the fit of the model is greatly improved by allowing a different intercept in each diversification phase. Of particular importance, slopes for individual regressions applied to data points within diversification phases are non-significant for Pennsylvanian–Triassic and Maastrichtian–Cenozoic, but are significant at  $p < 0.05$  for the Jurassic–Cretaceous (Supplementary Table 1).

## How sampling intensity influences maximum local richness estimates

*Simulated null distributions.* The simulations show that 1) per-bin maximum local richness will appear to increase through the Phanerozoic even if the underlying distribution remains constant (i.e., there is no change in local richness through time or space; Fig. 2); 2) richness curves based on the 90<sup>th</sup> percentile (a quantile of 0.9) are relatively robust to this sampling-opportunity bias (Fig. 2); and 3) a simulated null distribution using two underlying local richness pools (divided at the K/Pg boundary) fit the empirical data substantially better than a single Phanerozoic pool, and nearly as well as null distributions using larger numbers of underlying pools (Fig. 2; 3). This supports our interpretation of relative stasis in local richness prior to the K/Pg, followed by an abrupt two- to three-fold increase and continued stasis through the Cenozoic.

When simulating a null distribution using a single Phanerozoic pool of local richness values, maximum local richness appears to rise continuously and steeply through the Paleozoic, less steeply but erratically through the Mesozoic, and flattens out through the Cenozoic (Fig. 2). The empirical curve of per-bin maximum local richness lies largely below the lower confidence interval of the null distribution until the Cenozoic (Fig. 2). The null distribution for the 90<sup>th</sup> percentile (Fig. 2) is much flatter than for maximum local richness, although confidence intervals are considerably wider prior to the mid-Permian. The empirical curve for richness at the 90<sup>th</sup> percentile falls below the null prior to the K/Pg, but above the null during the Cenozoic.

In contrast, simulating a null distribution using two pools of local richness, separated at the K/Pg boundary, substantially improves the fit of the empirical data to the simulation, based on the sum of the squared residuals (Fig. 3). Although increases for per-bin maximum



local richness still spuriously appear to be continuous, there is a close correspondance between empirical and simulated richness curves at the 90<sup>th</sup> percentile. Until the mid-Permian, confidence intervals for richness at the 90<sup>th</sup> percentile are large for both empirical and simulated distributions. Adding a third underlying pool (either using era boundaries or diversification phases hypothesised on the basis of the empirical data) does not noticeably improve the fit of the empirical and simulated curves (Fig. 2). This suggests that the empirical data is most parsimoniously described by a two-phase pre- and post-K/Pg model of local richness, with relative stasis before and after. The artefactual increases or wide confidence intervals in the simulated distribution prior to the Permian suggest that it may be more difficult to infer local richness patterns during the earliest phase of tetrapod diversification, although exceptional localities such as Richard's Spur at least provide minimum bounds on local richness levels during this interval.

Our simulated null distributions show that the statistical support we recover for phase-shift models, based on fitting models to richnesses of exceptional localities, is conservative. This is because increases in sampling opportunities through time make it more likely that gradual increases would be favoured over phase-shift models, even if the underlying distribution of local richness was static.

*Rarefaction curves.* Rarefaction curves of non-flying tetrapod maximum local richness (Supplementary Fig. 5) broadly support our focal results. In particular, they show that 1) when controlling for the number of sampling opportunities, maximum local richness levels for non-flying tetrapods were very similar across the Paleogene, Neogene and Quaternary (rarefaction curves are nearly identical for most subsampling quotas); 2) that we cannot reject the possibility that maximum local richness did not change between the Jurassic and the Cretaceous; and 3) that Triassic, Permian and Carboniferous levels strongly overlap.

*Correlation analyses.* Maximum local richness per equal-length bin correlates strongly with counts of collections (Spearman's  $\rho = 0.85$ ,  $p = < 0.01$ ) and occupied grid-cells (Spearman's  $\rho = 0.8$ ,  $p = < 0.01$ ; Supplementary Figs 8a–b and 9a). However, correlations between the same variables are considerably weaker after they have been detrended using ARIMA models (counts of collections: Spearman's  $\rho = 0.48$  and  $p = < 0.01$ ; counts of occupied grid-cells: Spearman's  $\rho = 0.14$ ,  $p = 0.39$ ; Supplementary Figs 8c–d and 9b). This indicates that the raw relationships are driven by long-term trends of increase, and not by direct, short-term linkage. This is consistent with our interpretation of the link between sampling and maximum observed local richness, which is probabilistic but not additive. Nevertheless, poor sampling in some intervals of the Mesozoic (particularly in the Middle Jurassic and “mid”-Cretaceous) is coincident with (and likely related to) gaps in the record of exceptional fossil tetrapod localities, and this prohibits us from tracing a continuous time series of local richness through the Phanerozoic.

85

86       Patterns of local richness in major tetrapod clades

87       *Non-avian dinosaurs*: Local richness of non-avian dinosaurs was never high in  
88 comparison to small-bodied taxa such as mammals or squamates: remarkably, only 14  
89 localities through the entire Mesozoic have yielded more than 10 non-avian dinosaur genera.  
90 Maximum dinosaur richness per collection does not exceed five genera or seven species  
91 during the Triassic, but increased through the Jurassic, reaching 19 species/genera at the Dry  
92 Mesa Quarry collection of the Late Jurassic Morrison Formation, USA (Fig. 5a). With the  
93 exception of Careless Creek Quarry from the Judith River Formation (Campanian; 15  
94 species) and Lull 2 Quarry from the Lance Formation (Maastrichtian; 14 species) of the USA,  
95 local species richness of non-avian dinosaurs during the Late Cretaceous is notably lower  
96 than during the Late Jurassic. Patterns for formations are broadly congruent (Supplementary  
97 Fig. 2). Dinosaur richness increases gradually through the Triassic and Early Jurassic before  
98 reaching an apparent peak in the Late Jurassic (~62 species from the unusually vast and  
99 stratigraphically-thick Morrison Formation), and another in the Late Cretaceous (~51 species  
100 from the Dinosaur Park Formation in the Campanian; ~36 species from the Hell Creek and  
101 ~23 from the Lance in the Maastrichtian).

102       *Non-flying mammals*: Absolute counts of mammal taxa per collection are  
103 approximately twice those for non-avian dinosaurs (Fig. 5a and b). Sampled local richness of  
104 mammals increases gradually from their origins in the Late Triassic to the Middle Jurassic,  
105 before reaching an apparent Mesozoic maximum during the Late Jurassic. Kimmeridgian–  
106 Tithonian localities that have been bulk-sampled, such as Guimarota and Quarry 9, Como  
107 Bluff, are at least as rich (~33 species) as the richest localities from the Early Cretaceous  
108 (~26 species from the Mammal Bed, Durlston Bay (Lulworth Formation, UK; Berriasian)  
109 and Maastrichtian (~25 species from Bushy Tailed Blowout and Lull 2 Quarry from the

Lance Formation, and Flat Creek 5 from the Hell Creek Formation; Fig. 5b). However, counts of genera per collection are similar between the Late Jurassic and Maastrichtian, and richness per formation may be higher in the Maastrichtian.

Richness per collection and formation both suggest that mammals on a global level experienced a sharp two-to-three-fold increase in local richness across the K/Pg boundary (Fig. 5b, Supplementary Figs 1c and 2c), consistent with previous findings for North America<sup>1-3</sup>. Maximum local richness subsequently fluctuated around ~60 species per collection throughout the Cenozoic. Even the large increase in the prevalence of cave deposits in the Plio-Pleistocene does not appear to result in a noticeable increase. This is consistent with sampling-standardized analyses of continental-scale diversity in North American land-mammals<sup>4,5</sup>. Excepting the Miocene-aged Norden Bridge Quarry (Valentine Formation, Langhian; 77 species), richness of mammals per collection peaked in the Paleocene–Eocene and dropped during the Oligocene. Counts of mammal species per formation also drop dramatically, halving from the late Paleogene into the Neogene. A mid-Cenozoic decline in local richness of North American mammals was previously reported by Stucky<sup>6</sup>. This decline may be linked to the deterioration of global climatic conditions (particularly in North America, the continent that contributes the strongest signal to the “global” pattern). Global cooling is thought to have driven the Bridgerian Crash in North American mammalian diversity at local and continental scales around 50–47 Ma<sup>7</sup>.

*Squamates*: Squamate local richness remained very low (no more than 5–8 species per collection) from their earliest appearance in the fossil record, during the Early–Middle Jurassic, until the Campanian, when counts more than doubled (~19 species from Ukhaa Tolgod, Djadokhta Formation, and ~17 species from Khulsan, Barun Goyot Formation; Fig. 5c; Supplementary Fig. 1d). There is no clear evidence for face-value increases immediately across the K/Pg boundary. In fact, squamates appear to have been substantially affected by

the extinction: during the Paleocene, richness dropped to no more than 11 species per collection. However, by the Ypresian, maximum squamate local richness had once again attained Late Cretaceous levels. These levels (maximally ~20–28 species) broadly persisted until the end of the Cenozoic. Patterns of squamate richness per formation are congruent with counts of taxa per collection, but there is a pronounced peak in richness per formation during the Campanian (Supplementary Fig. 2d and g).

*Pseudosuchians, turtles and lissamphibians:* Ecologically important and abundant but species-poor groups such as pseudosuchians (crocodylians and their stem-group) and turtles show overwhelmingly flat local richness levels throughout much of their evolutionary histories (Supplementary Fig. 18). Pseudosuchian local richness peaked in the Late Triassic, followed by remarkable stasis through the remainder of the Mesozoic. This trend continues through the Cenozoic, until a second peak is reached in the late Miocene. Turtle local richness saw apparent peaks in the Maastrichtian and Ypresian, followed by a slight decline towards the present. However, it is often difficult to diagnose pseudosuchian and turtle species from fragmentary material, and this may depress their sampled richness outside of Lagerstätten-style deposits. Sampled lissamphibian local richness is also low. However, given their high diversity today, this is more likely to be due to low preservation potential or diagnosability. Although very low for most of the Mesozoic, there is an apparent rise in lissamphibian local richness during the well-sampled Maastrichtian. Unlike other major groups, lissamphibian local richness does not increase consistently during the Cenozoic.

*Flying tetrapods:* The diversity dynamics of flying tetrapods in deep time are more difficult to establish. Due to their fragile skeletons, our ability to trace patterns of local richness in birds, bats and pterosaurs depends much more heavily on rare events of exceptional preservation, such as Konservat-Lagerstätten deposits. Nevertheless, a small handful of truly exceptional sites allow us to draw preliminary conclusions about patterns of

local richness in flying tetrapods. We focus on counts of flying taxa per formation, because collections in crucial deposits (such as those from the Early Cretaceous Jehol Group in China, where most fossils are collected by local farmers and precise origins are usually unknown) are geographically over-split, artificially deflating richness estimates. We have selectively updated records for key deposits using counts of species from the literature, because data entry in the PaleoDB for flying tetrapods is currently incomplete.

Our results tentatively suggest that maximum local richness of flying tetrapods increased surprisingly little from the Cretaceous to the Neogene (Supplementary Fig. 15). From the Early Cretaceous of China, 66 flying tetrapod species are known from the Jiufotang Formation (including ~46 birds) and 41 from the Yixian Formation (including ~24 birds), although there may be problems with taxonomic oversplitting in the Mesozoic. By contrast, 77 flying tetrapod species are known from the Lutetian-aged (Paleogene, Cenozoic) Messel deposits, where birds and bats are known from hundreds of virtually complete specimens<sup>8</sup>. Fifty-six named species of bird are known from Messel, and an informal tally including undescribed specimens elevates this number to 70 species<sup>9</sup>. At least 36 species are known from the lower Eocene Green River Formation, USA [including ~34 birds; <sup>10</sup>].

Local richness of flying taxa appears to have increased very little between the early Cenozoic and the Recent. The proportional representation of birds and bats within localities and formations increases spectacularly in the Plio-Pleistocene (Supplementary Fig. 15a and b; 15e–h), caused by dramatic increases in the availability of caves and geologically short-lived depositional contexts (see above; Supplementary Fig. 7). In spite of this taphonomic bias, the spectacular avian local richness at Messel is on par with that of even the richest late Cenozoic deposits: only two Pliocene–Holocene formations exceed 30 species, and only one exceeds Messel in richness (the Pliocene Yorktown Formation, USA, with 87 species). For comparison, eBird (<http://www.ebird.org/>) suggests present-day avian local richness hotspots

range from 70–130 species. Bat local richness is also highly constrained, being maintained at ~10 species from their initial appearance in the early Eocene until the Recent (Supplementary Fig. 15c)<sup>11,12</sup>.

#### Patterns of non-flying tetrapod richness per formation during the Mesozoic

Were it not for three exceptionally diverse formations, the Morrison Formation in the Late Jurassic and the Hell Creek and Lance formations in the Maastrichtian, we might conclude that maximum richness per formation did not increase from the Triassic to the mid-Cretaceous, before increasing in the Late Cretaceous. Counts of species and genera from the Morrison Formation are at least twice those of any other Jurassic formation. However, the outlier status of the Morrison Formation is likely to result from the fact that it is geographically vast (~1.5 million square km), extending from New Mexico to Montana and encompassing a large variety of paleoenvironments, stratigraphically thick (~50 m), and because it has been intensively sampled for over 100 years<sup>13</sup>. The Hell Creek and Lance formations are 1.5-fold richer than the next richest Cretaceous formations (Djadokhta and Barun Goyot, East Asia; crucially, however, these formations have not been bulk-sampled), and comparable to the Late Jurassic Morrison Formation. We therefore consider it possible that this apparent 1.5-fold increase is the result of more intense sampling during the Maastrichtian, and in particular the increasing importance of isolated mammal teeth obtained by intensive bulk-sampling, as well as more intense taxonomic scrutiny and higher diagnosability of those remains that are collected.

#### Patterns of local richness within continental regions

Patterns of local richness in Phanerozoic tetrapods are broadly congruent between the patterns derived from the aggregated global data and those for individual continental regions (Supplementary Fig. 17). This is because pooled “global” patterns are strongly driven by North America and Europe, the two continental regions that have historically been best-sampled. North America contributes the most data for many important intervals, including the Permian, Late Cretaceous and Paleogene. All of the key events in Phanerozoic local tetrapod richness are recorded in North America, including the late Carboniferous rise, Permo-Triassic stasis, Jurassic and Maastrichtian increases, and Cenozoic stasis. However, gaps are present in the North American record during the Devonian–Mississippian, Late Permian, Middle Jurassic and Early Cretaceous. Europe corroborates the late Carboniferous rise, Jurassic increase and, to some extent, Cenozoic stasis (although the early Paleogene record is poor). Substantial gaps exist in the European record for the Permo-Triassic, “mid”-Late Cretaceous and early Paleogene.

Records of local richness for other continental regions are much less complete. The South American record is poor prior to the Cenozoic, and the Neogene is better-sampled than the Paleogene. Africa and Asia contribute global maxima in local richness across the Permo-Triassic boundary. Asian localities contribute to global maxima in local richness in the Late Cretaceous (e.g. Ukhaa Tolgod, Campanian). However, aside from one collection in the Early Cretaceous (Ksar Met-Lili, Anoual), African localities do not affect global maxima until the Neogene and Quaternary. With some exceptions (e.g. Riversleigh in Queensland, Australia), geographic regions encompassing equatorial paleolatitudes (including those not contained within our five continental regions; designated in Supplementary Fig. 17 as “Other”) do not contribute substantial amounts of data on tetrapod local richness until the Neogene–Quaternary (Supplementary Fig. 16).

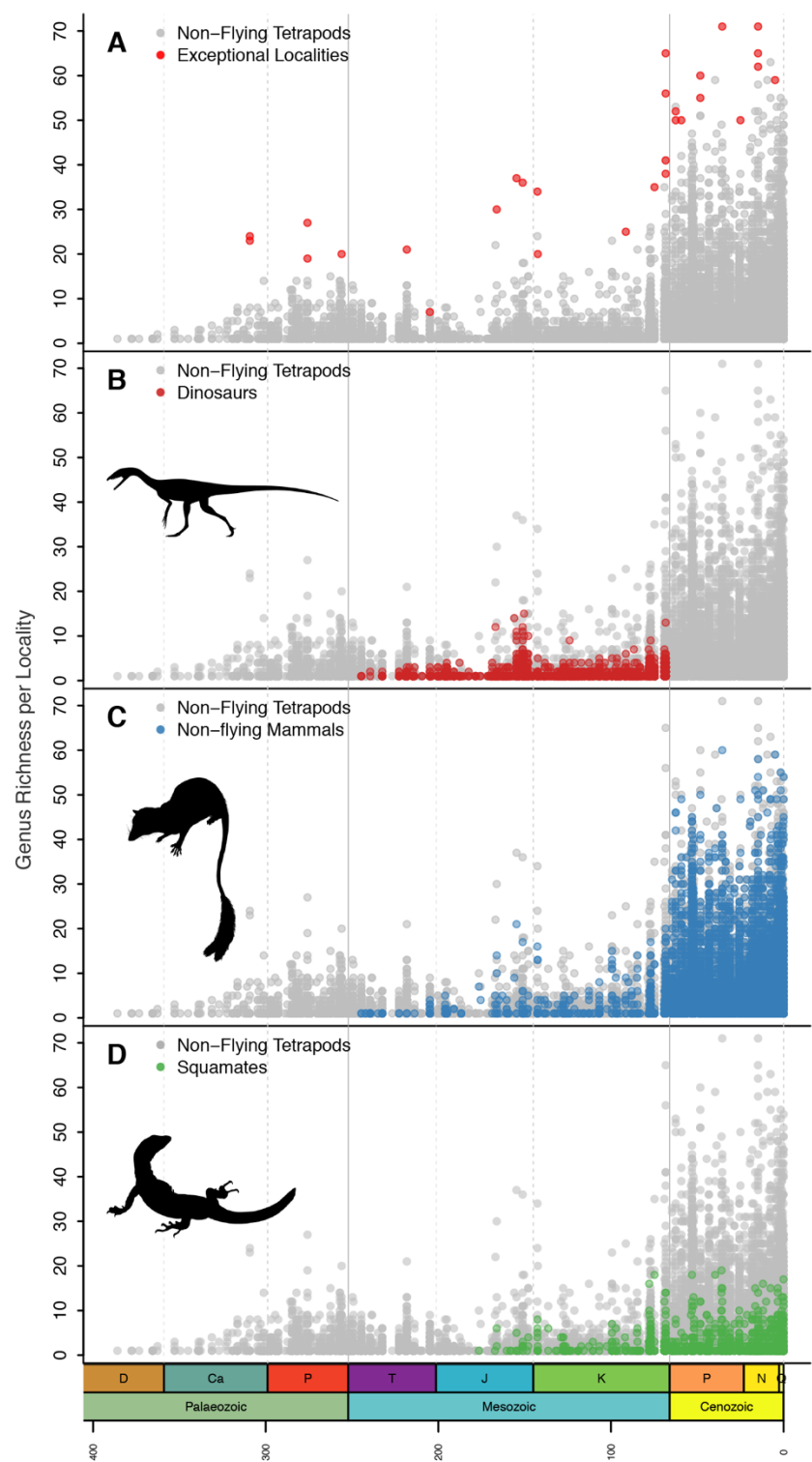


Supplementary Fig. 16 could be interpreted as showing a geographic shift in peak local richness from mid to low paleolatitudes through the latter half of the Cenozoic (perhaps due to the establishment of a modern-style latitudinal diversity gradient). However, this is more likely to be a sampling artefact resulting from the marked increase in the number of localities known from low paleolatitudes in the Neogene and Quaternary (Supplementary Fig. 19).

### Supplementary References

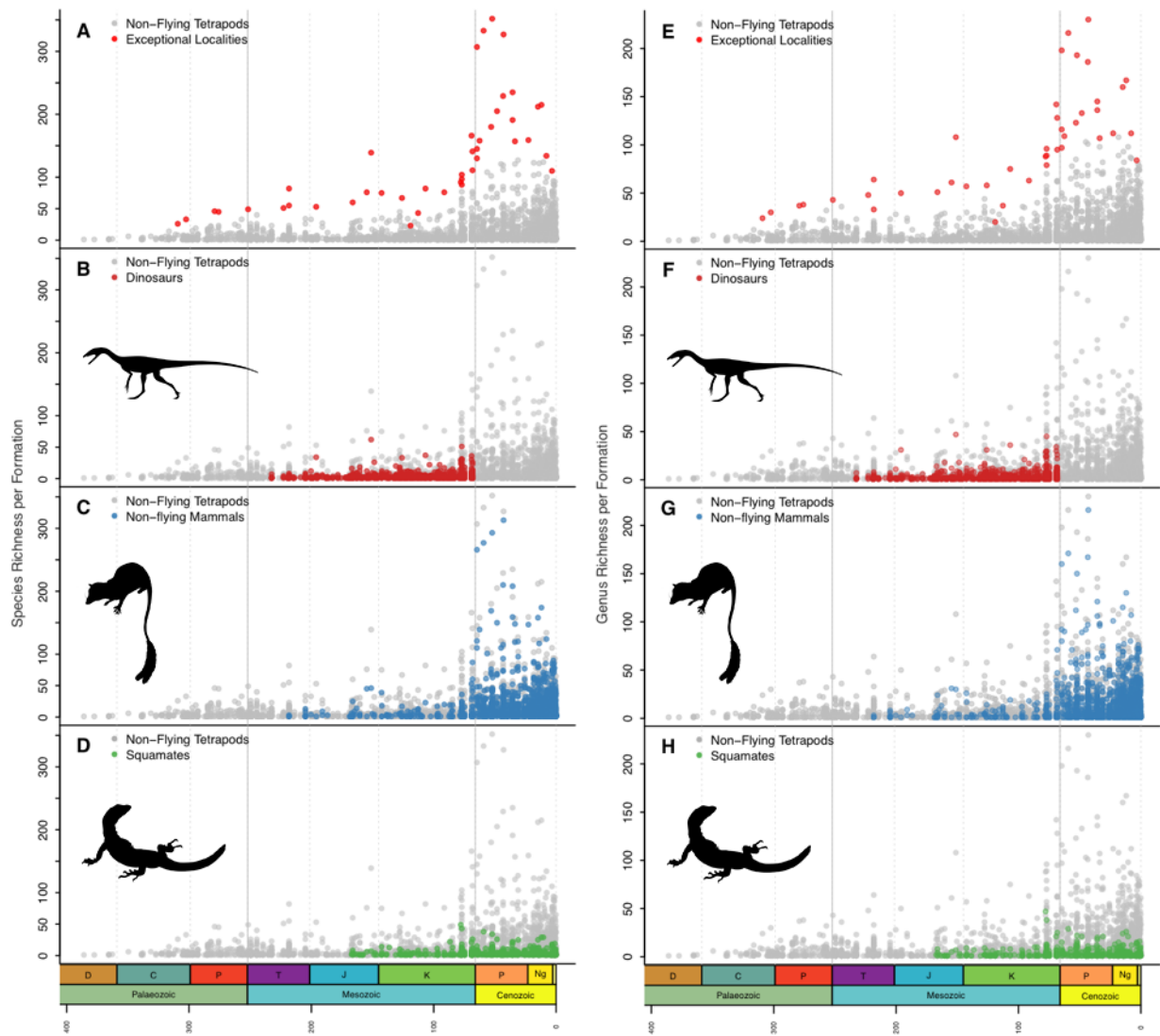
1. Cifelli, R. L., Eberle, J. J., Lofgren, S. E., Lillegraven, J. A. & Clemens, W. A. in *Late Cretaceous and Cenozoic Mammals of North America* (ed. Woodburne, M. O.) 21–42 (Columbia University Press, 2004).
2. Wilson, G. P. Mammals across the K/Pg boundary in northeastern Montana, U.S.A.: dental morphology and body-size patterns reveal extinction selectivity and immigrant-fueled ecospace filling. *Paleobiology* **39**, 429–469 (2013).
3. Wilson, G. P. in *Through the End of the Cretaceous in the Type Locality of the Hell Creek Formation in Montana and Adjacent Areas* **503**, 365–392 (Geological Society of America, 2014).
4. Alroy, J. in *Biodiversity Dynamics* (eds. McKinney, M. L. & Drake, J. A.) (Columbia University Press, 1998).
5. Alroy, J., Koch, P. L. & Zachos, J. C. Global climate change and North American mammalian evolution. *Paleobiology* **26**, 259–288 (2000).
6. Stucky, R. K. in *Current Mammology* **2**, 375–432 (1990).
7. Woodburne, M. O. & Gunnell, G. F. Climate directly influences Eocene mammal faunal dynamics in North America. *PNAS* **106**, 13399–13403 (2009).
8. Franzen, J. L. in *Eocene Biodiversity* (ed. Gunnell, G. F.) **18**, 197–214 (Springer, Boston, MA, 2001).
9. Mayr, G. The early Eocene birds of the Messel fossil site: a 48 million-year-old bird community adds a temporal perspective to the evolution of tropical avifaunas. *Biol. Rev.* **92**, 1174–1188 (2016).
10. Grande, L. *The Lost World of Fossil Lake*. (University of Chicago Press, 2013).  
doi:10.7208/chicago/9780226922980.001.0001
11. Storch, G. in *Eocene Biodiversity* (ed. Gunnell, G. F.) **18**, 215–235 (Springer US, 2001).

- 260 12. Archer, M. *et al.* Current status of species-level representation in faunas from selected fossil localities in  
261 the Riversleigh World Heritage Area, northwestern Queensland. *Alcheringa* **30**, 1–17 (2006).
- 262 13. Turner, C. E. & Peterson, F. Reconstruction of the Upper Jurassic Morrison Formation extinct  
263 ecosystem—a synthesis. *Sedimentary Geology* **167**, 309–355 (2004).
- 264

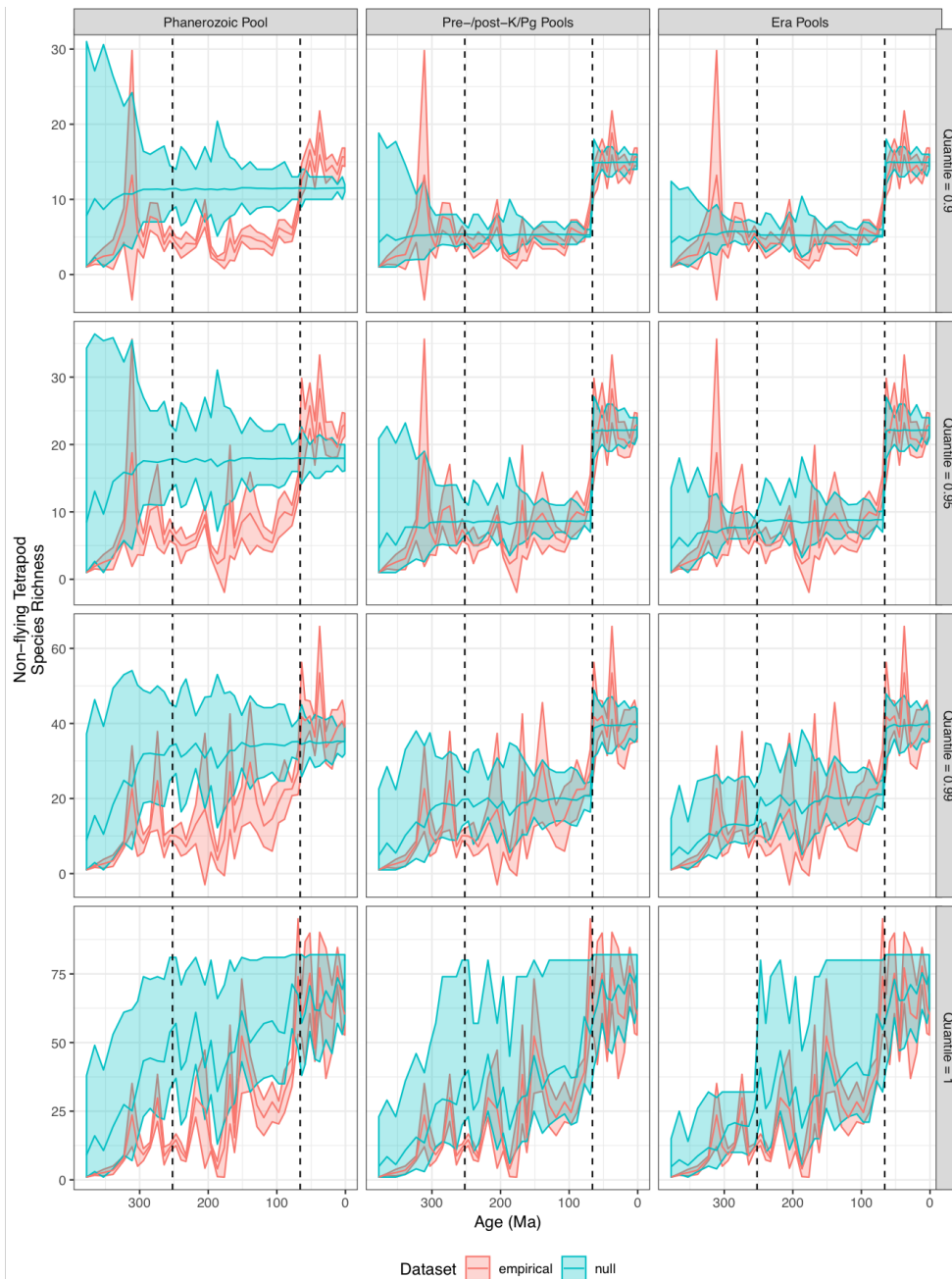


266

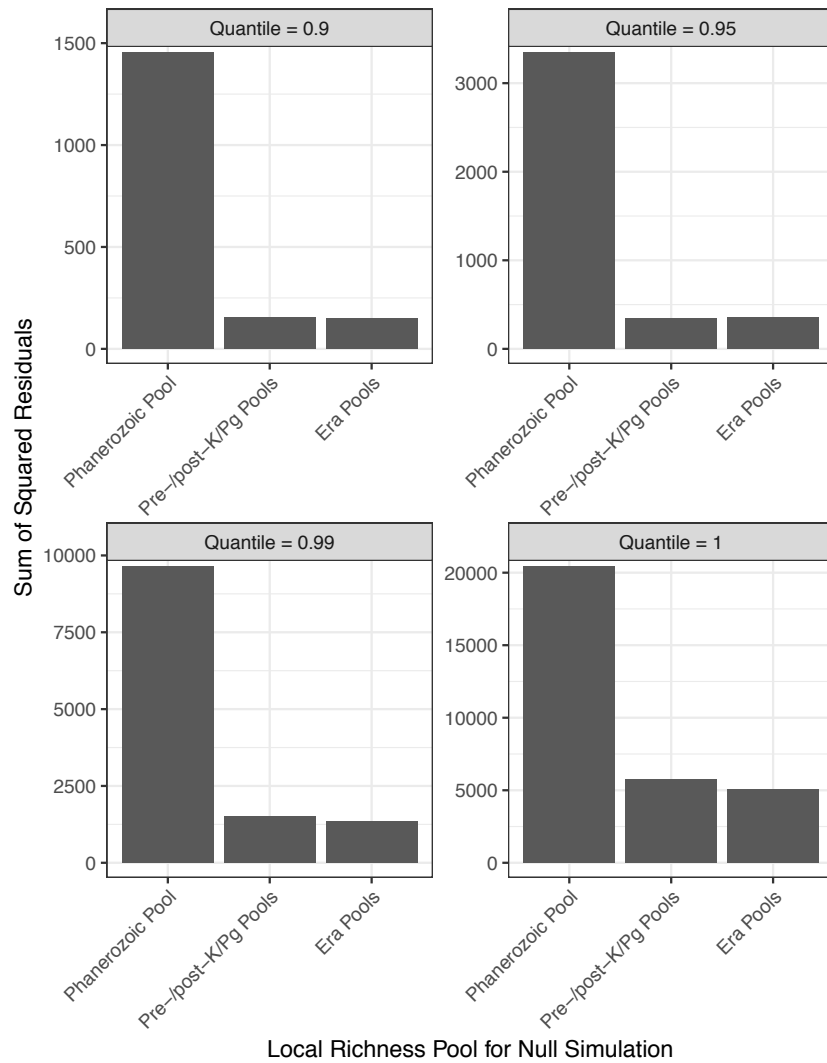
267 **Supplementary Fig. 1.** Genus-level local richness (taxa per collection) for non-flying, non-  
268 marine Phanerozoic tetrapods. **a**, Non-flying, non-marine tetrapods. **b**, Non-avian dinosaurs.  
269 **c**, Non-chiropteran mammalianomorphs. **d**, Squamates.



**Supplementary Fig. 2.** Richness per formation for Phanerozoic non-flying terrestrial tetrapods. Species richness for **a**, Non-flying tetrapods. **b**, Non-avian dinosaurs. **c**, Non-chiropteran mammaliamorphs. **d**, Squamates. Genus richness for **e**, Non-flying tetrapods. **f**, Non-avian dinosaurs. **g** Non-chiropteran mammaliamorphs. **h**, Squamates.



**Supplementary Fig. 3.** Comparison between the empirical curve of local species richness (using quantiles of 0.9, 0.95, 0.99 and 1) for terrestrial tetrapods and simulated null distributions. Richness quantiles calculated for equal-length bins.



279

280

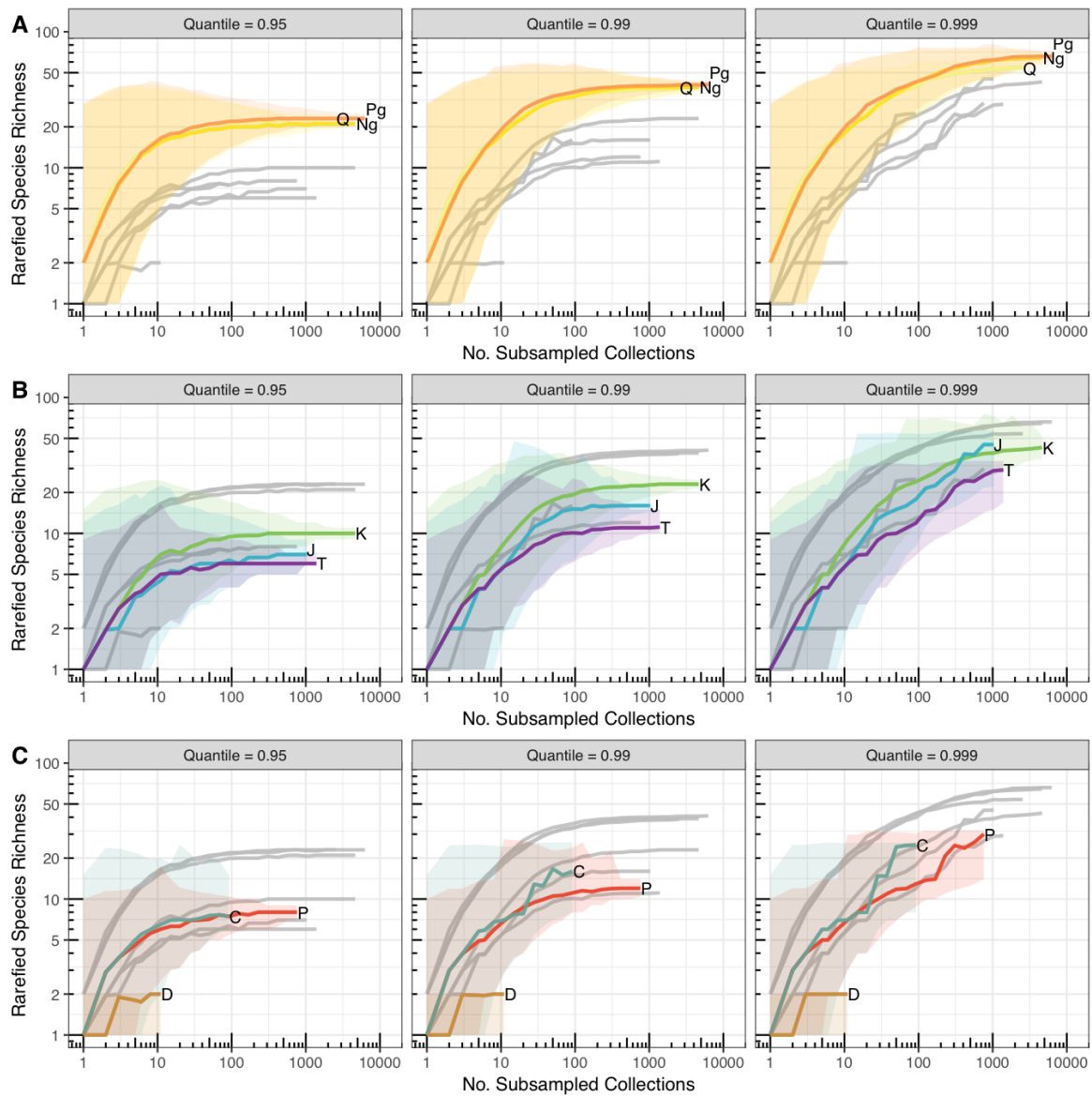
281

282

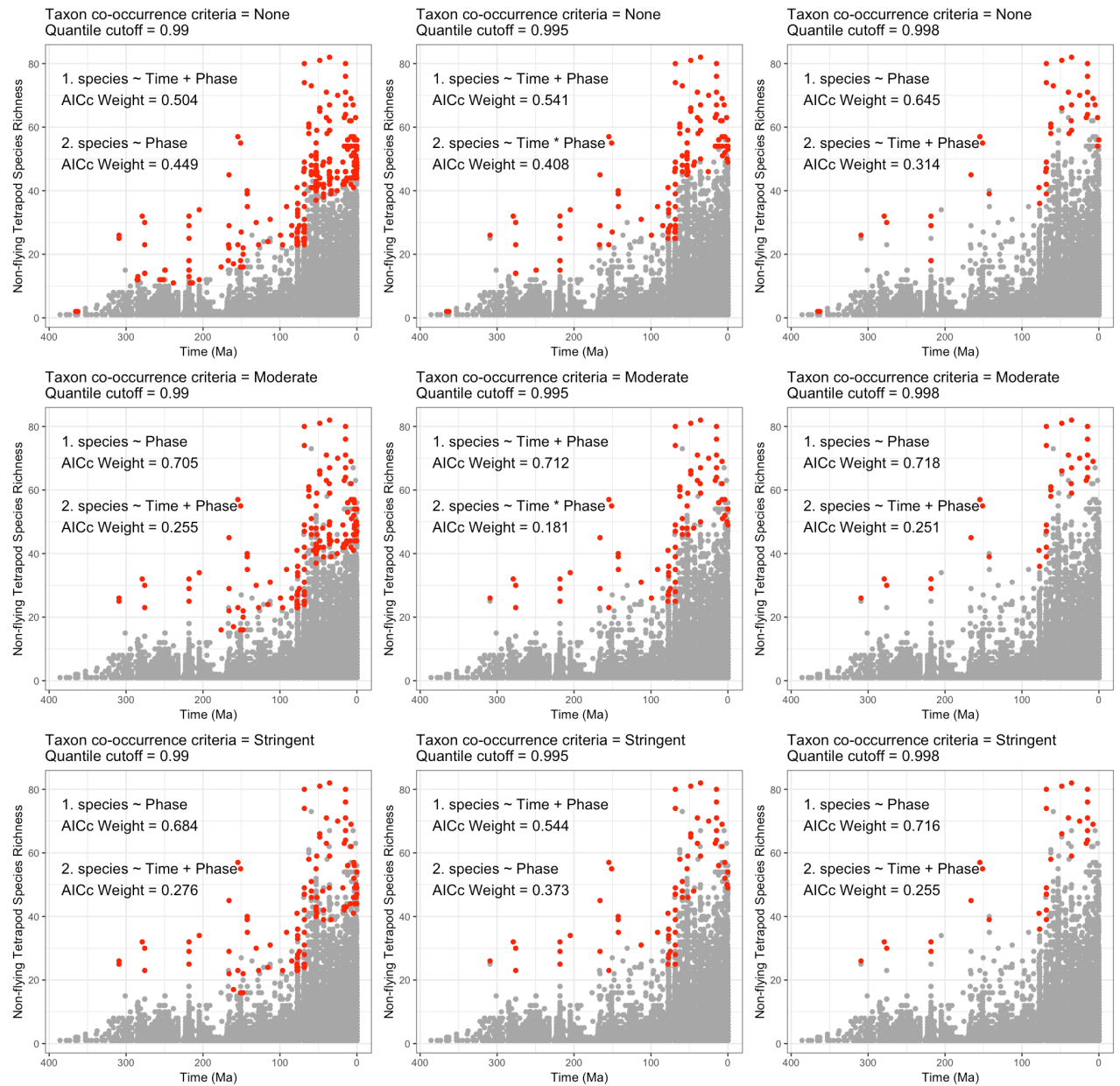
283

284

**Supplementary Fig. 4.** Residual sums of squares for simulated null distributions of local richness (using quantiles of 0.9, 0.95, 0.99 and 1) using Phanerozoic, Pre-/Post-K/Pg and Era Pools. Using separate pre-/post-K/Pg pools substantially improves the fit compared to a single Phanerozoic pool, while adding a third pool (Era Pools) makes only a negligible improvement.

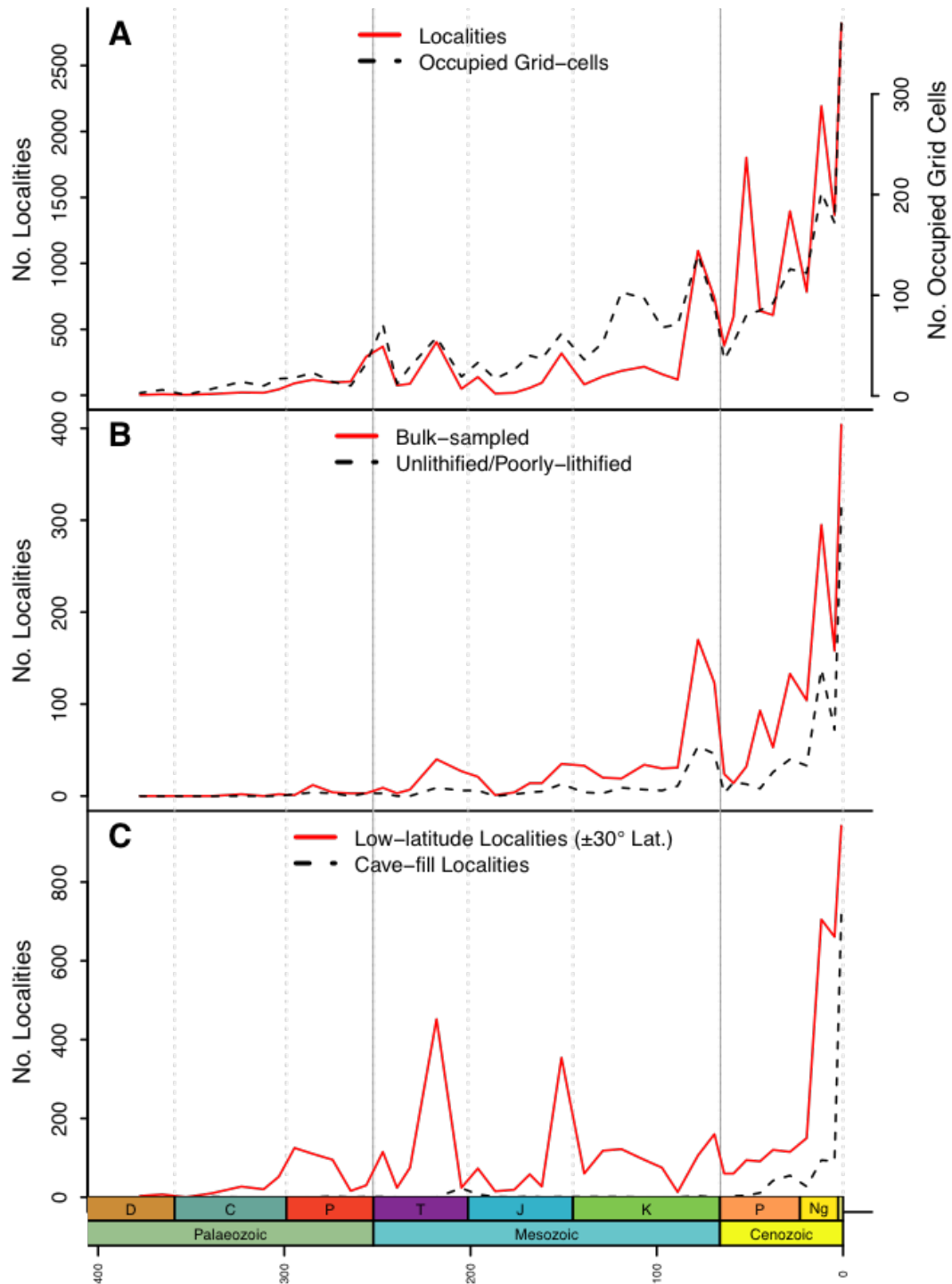


**Supplementary Fig. 5. Rarefaction curves for local richness quantiles of terrestrial tetrapods, rarefying by collection.** Shaded regions show 95% confidence intervals calculated by bootstrapping (1000 replicates). **a**, Cenozoic. **b**, Mesozoic. **c**, Palaeozoic.

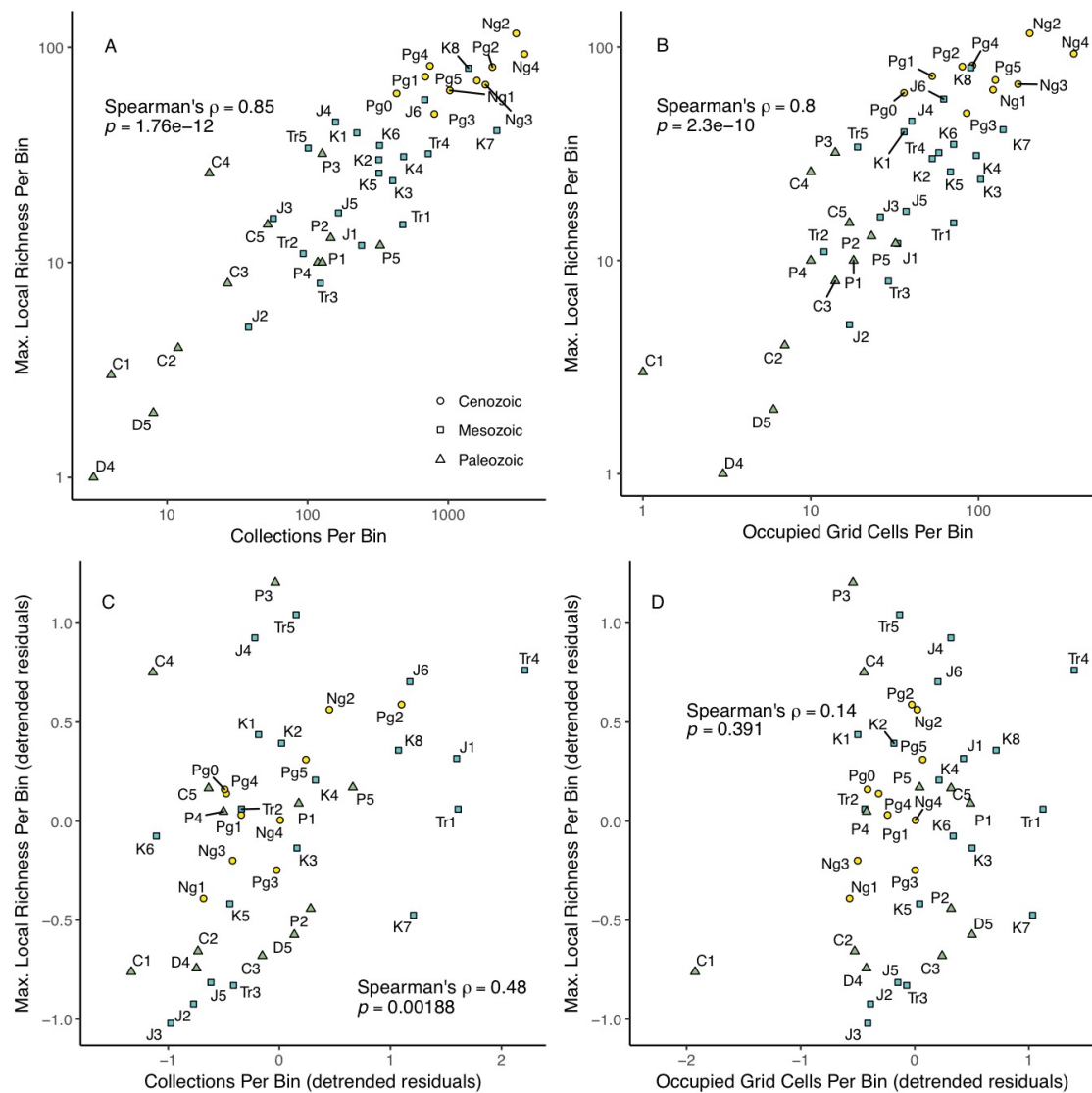


**Supplementary Fig. 6.** Localities selected using numerical definitions of exceptional sites (combining taxonomic co-occurrence criteria with quantile thresholds). See Methods for details.

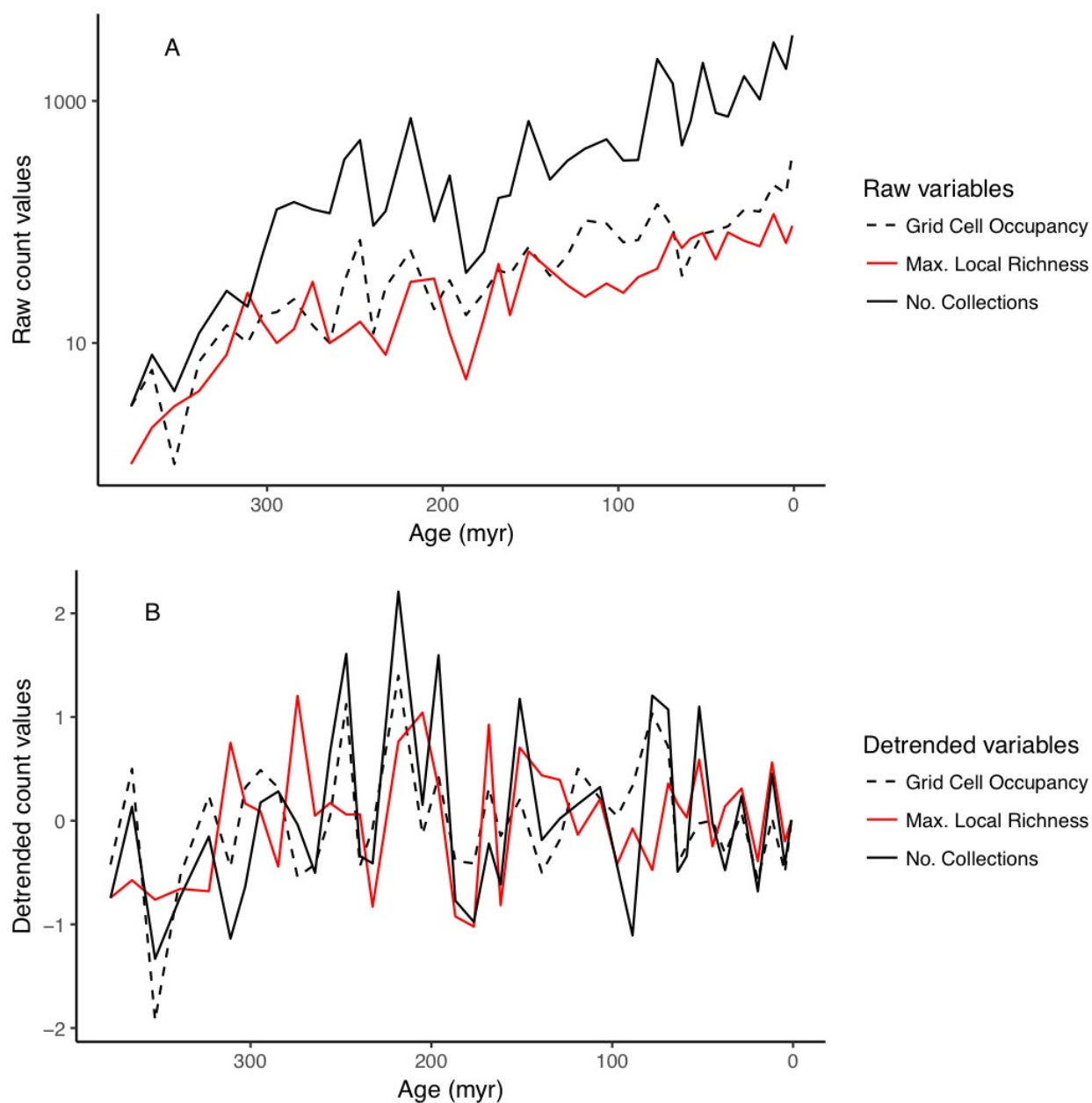




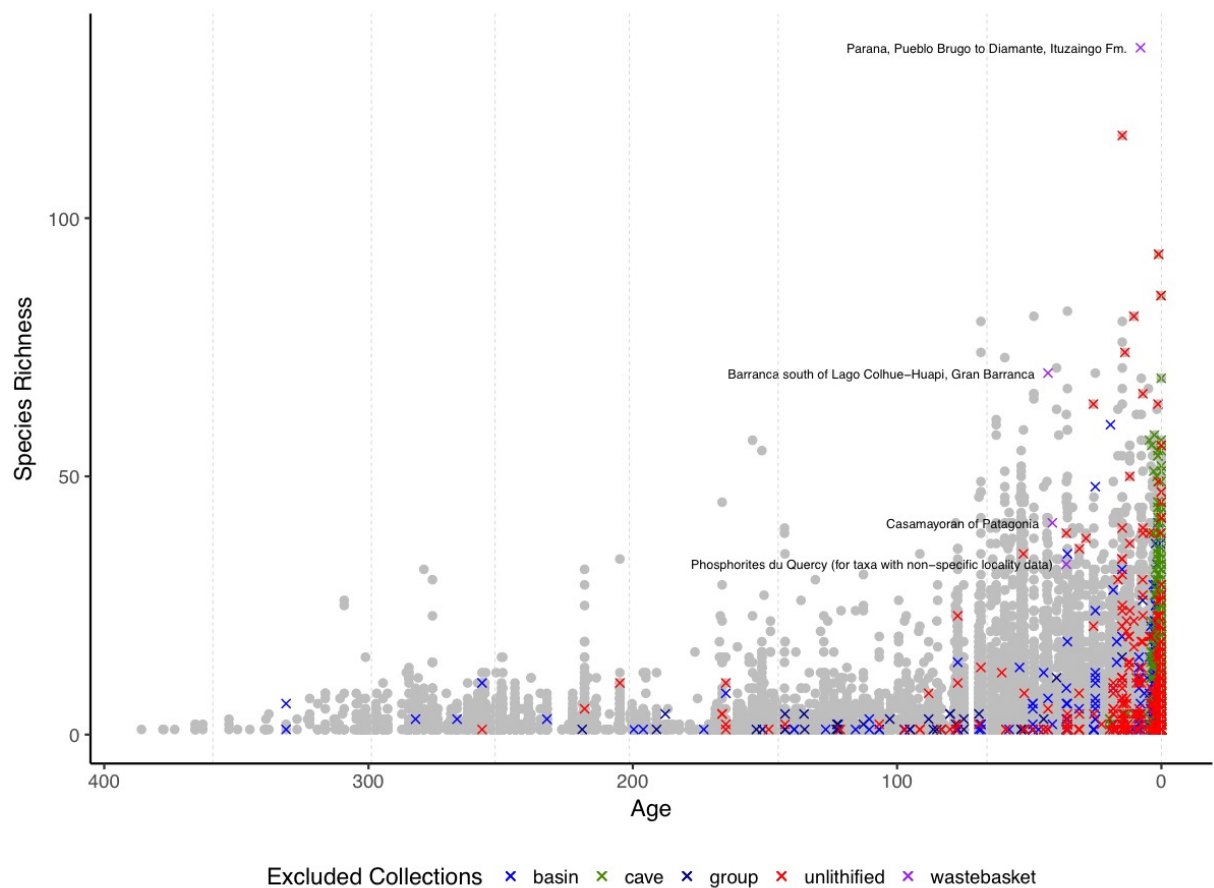
**Supplementary Fig. 7.** Sampling trends in Phanerozoic tetrapods. **a**, Counts of collections and occupied equal-area grid cells (50 km spacing). **b**, Counts of bulk-sampled and unlithified or poorly-lithified collections. **c**, Counts of low-palaeolatitude collections (within  $\pm 30^\circ$  of palaeolatitude either side of the palaeoequator) and cave-fill collections.



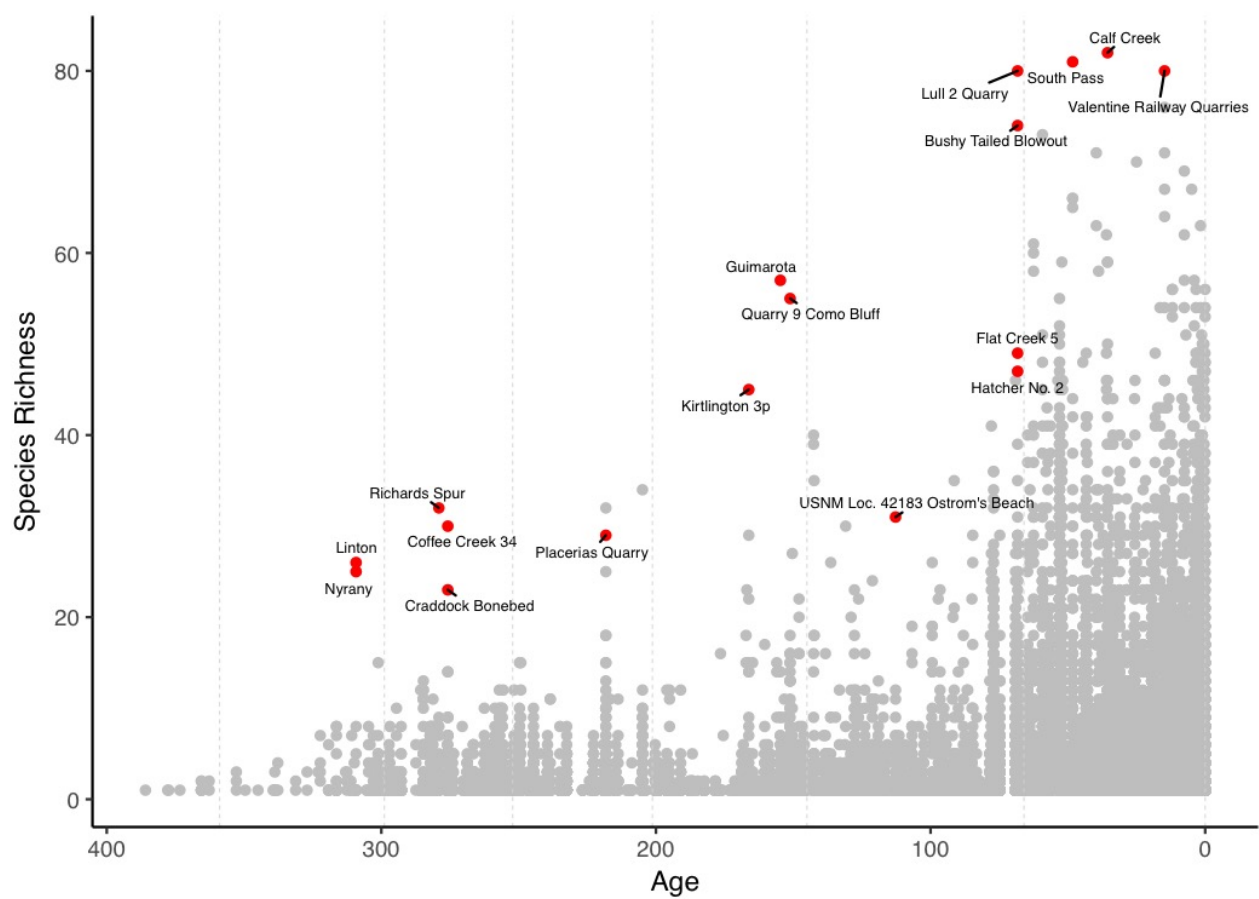
**Supplementary Fig. 8.** Correlation between maximum local richness of non-flying tetrapods and sampling proxies. Points represent equal-length bins. **a**, Raw relationship between maximum local richness of non-flying tetrapods and counts of collections. **b**, Raw relationship between maximum local richness of non-flying tetrapods and counts of occupied equal-area grid cells with 50 km spacings. **c**, Relationship between maximum local richness of non-flying tetrapods and counts of collections after applying first-differencing. **d**, Relationship between maximum local richness of non-flying tetrapods and counts of occupied equal-area grid cells with 50 km spacings after applying first-differencing. First differencing aggressively removes the influence of long-term correlations, so that only short-term correlations remain.



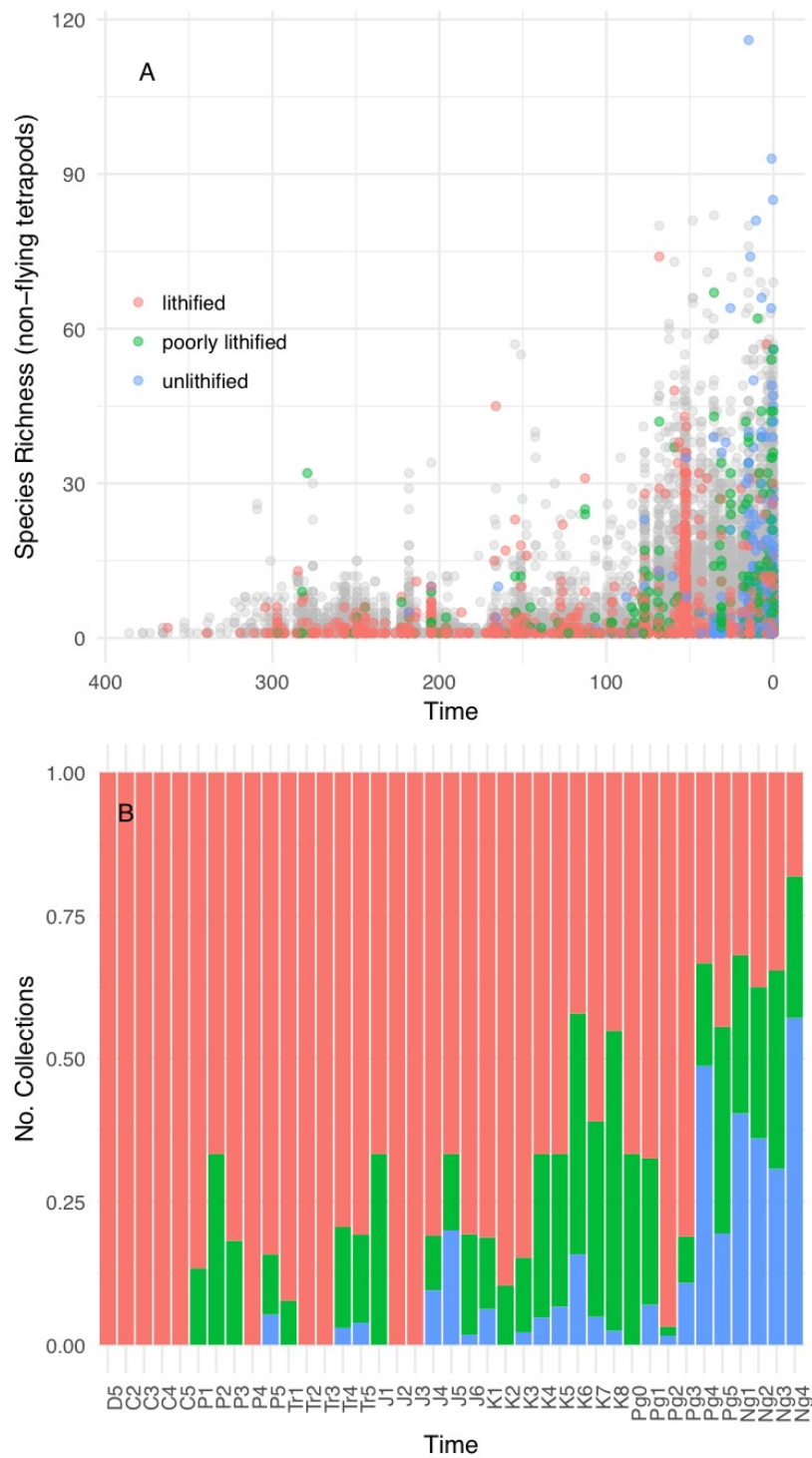
**Supplementary Fig. 9. a, Raw and b, model-detrended time series of sampling proxies and local richness.**



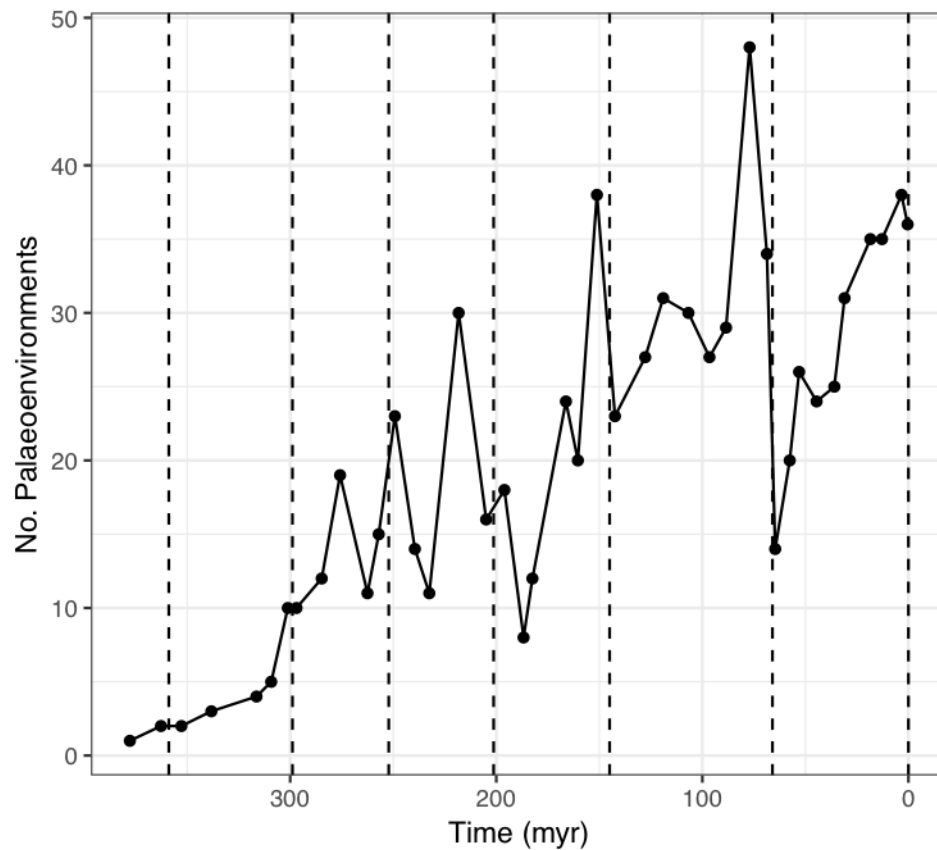
**Supplementary Fig. 10.** Collections that have been dropped from main figures and analyses, either because they represent “wastebasket” collections in the Paleobiology Database; preservation conditions that are difficult to compare with earlier parts of the fossil record (unlithified sediments, cave-fill environments); basin-level geographic scales; or group-level stratigraphic scales.



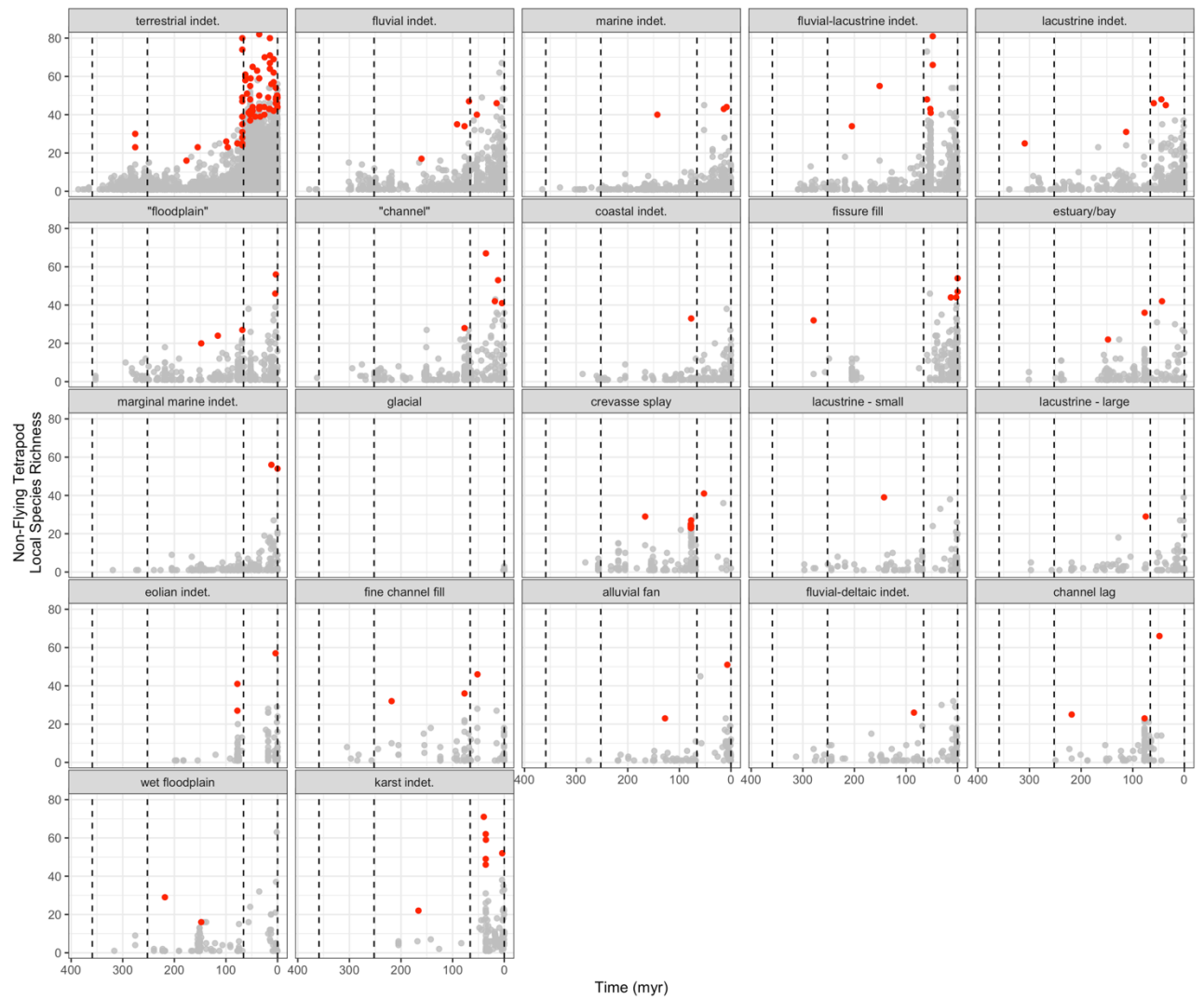
**Supplementary Fig. 11.** Identities of selected exceptional localities through the Phanerozoic.



**Supplementary Fig. 12.** Proportions of lithified, unlithified and poorly lithified collections through time. **a**, Local richness for Phanerozoic non-marine tetrapods, colored by lithification category. **b**, proportions of lithified, poorly-lithified and unlithified collections through time.

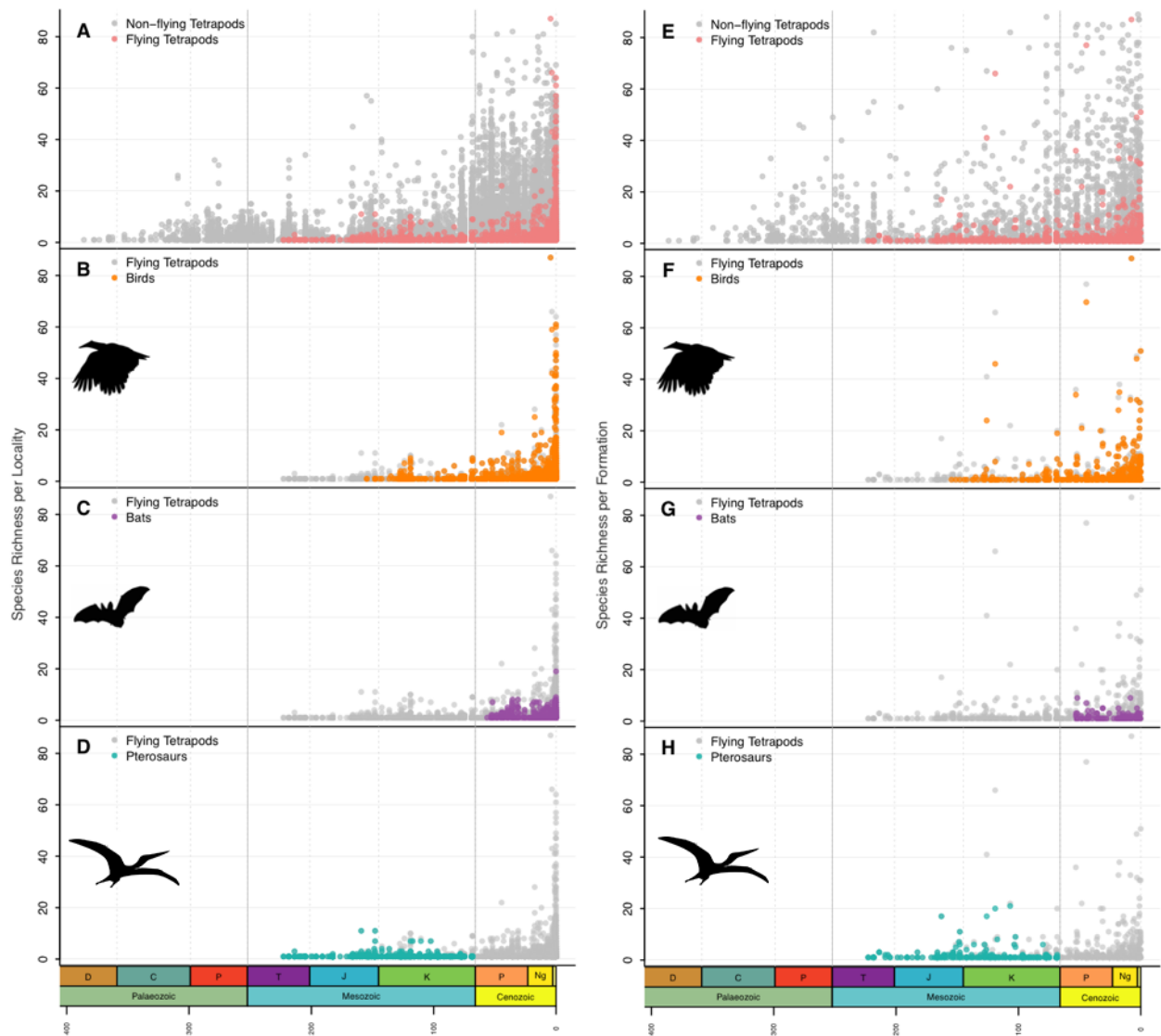


**Supplementary Fig. 13.** Counts of distinct environments (as recorded in the Paleobiology Database) per equal-length bin. The diversity of sampled environments within localities rose steadily through the Paleozoic–Mesozoic before falling across the K/Pg. Despite this, local richness rose abruptly in the Cenozoic, suggesting that sampled environments are not contributing to the broad Phanerozoic pattern of local richness.

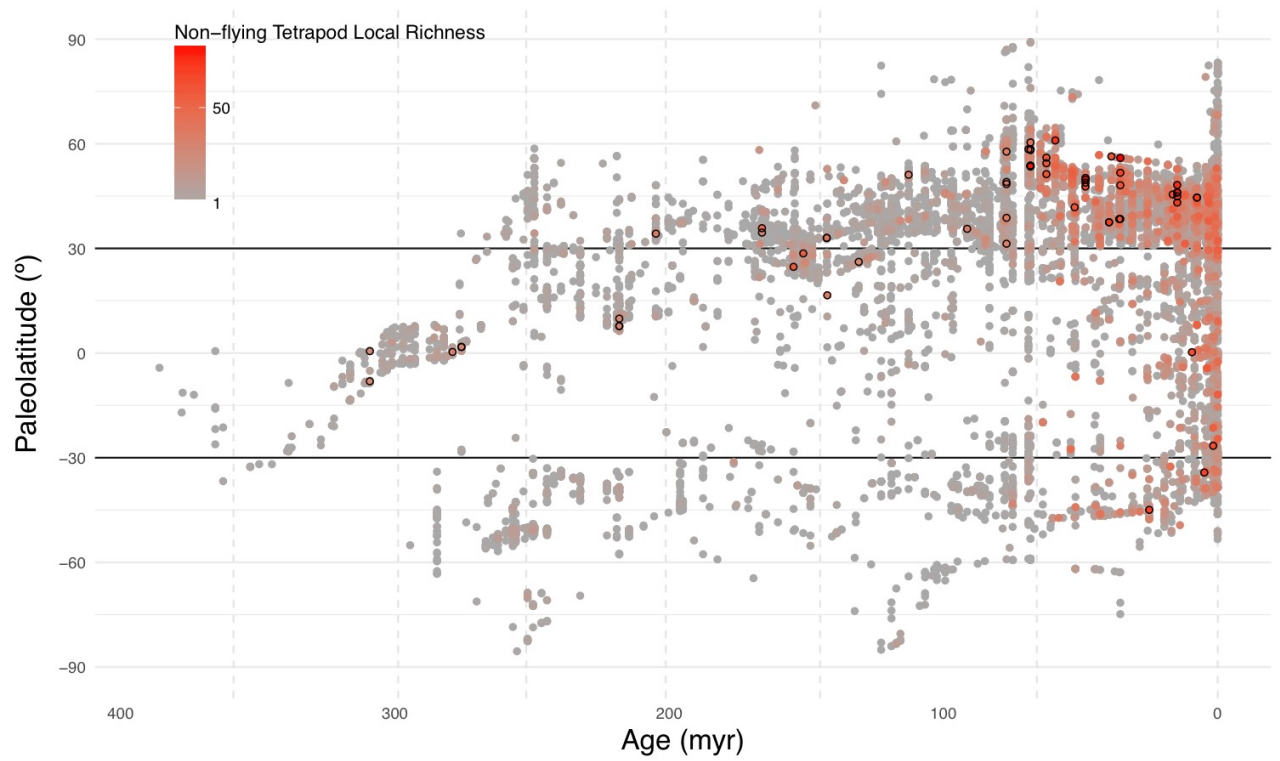


**Supplementary Fig. 14.** Patterns of local richness within environmental types, as classified in the Paleobiology Database. Red points indicate exceptional localities (taxonomic co-occurrence restrictions = moderate, quantile cutoff = 0.99). Exceptional localities derive from a wide range of environment types, and exhibit no obvious temporal bias. Standardising for environmental type is difficult because most collections in the Paleobiology Database are recorded as “terrestrial indet.” due to limits of reporting in the palaeontological literature.

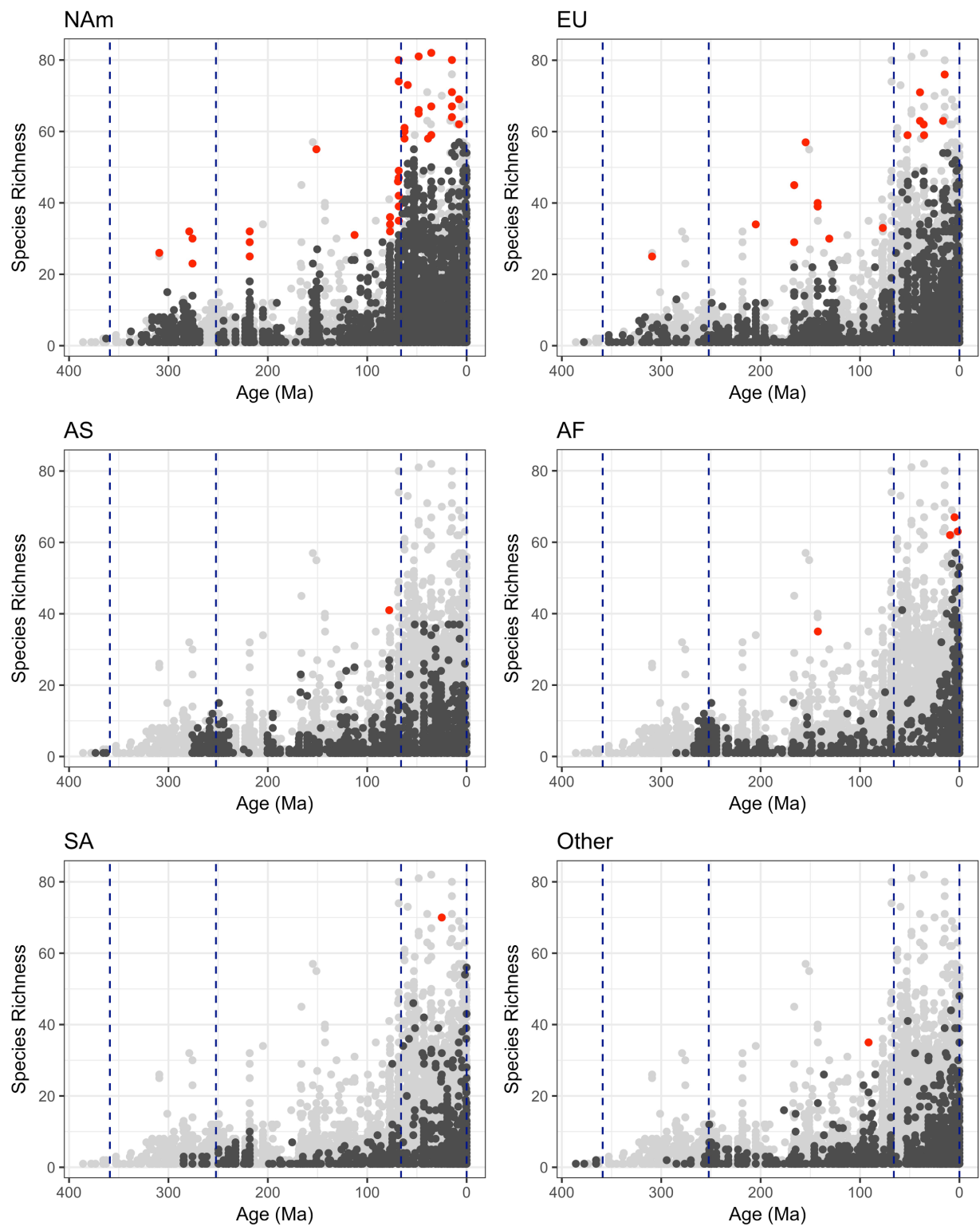




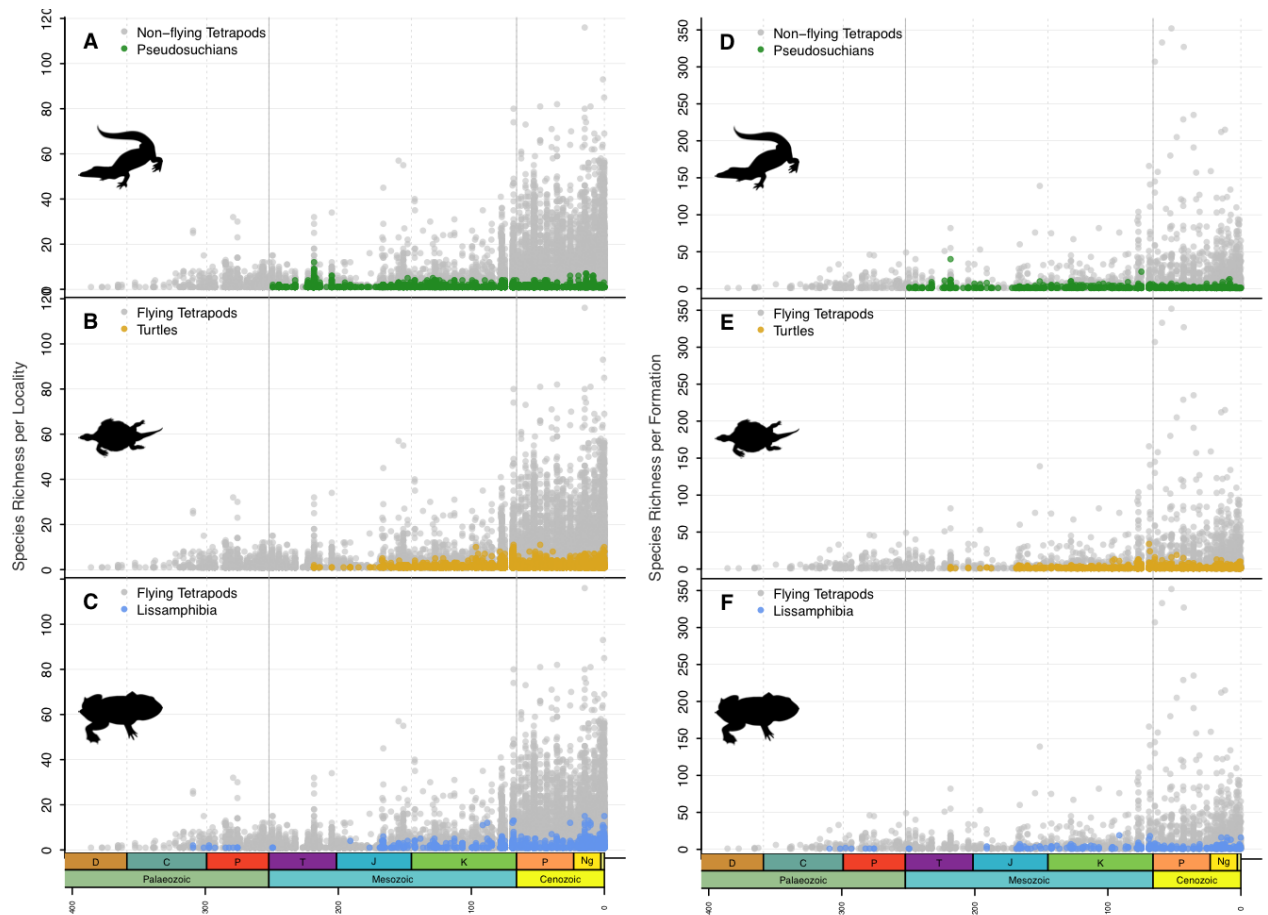
**Supplementary Fig. 15.** Local species richness for Phanerozoic flying tetrapods. Species per collection for **a**, Flying tetrapods contrasted against non-flying tetrapods. **b**, Birds. **c**, Bats. **d**, Pterosaurs. Species per formation for **e**, Flying tetrapods contrasted against non-flying tetrapods. **f**, Birds. **g**, Bats. **h**, Pterosaurs.



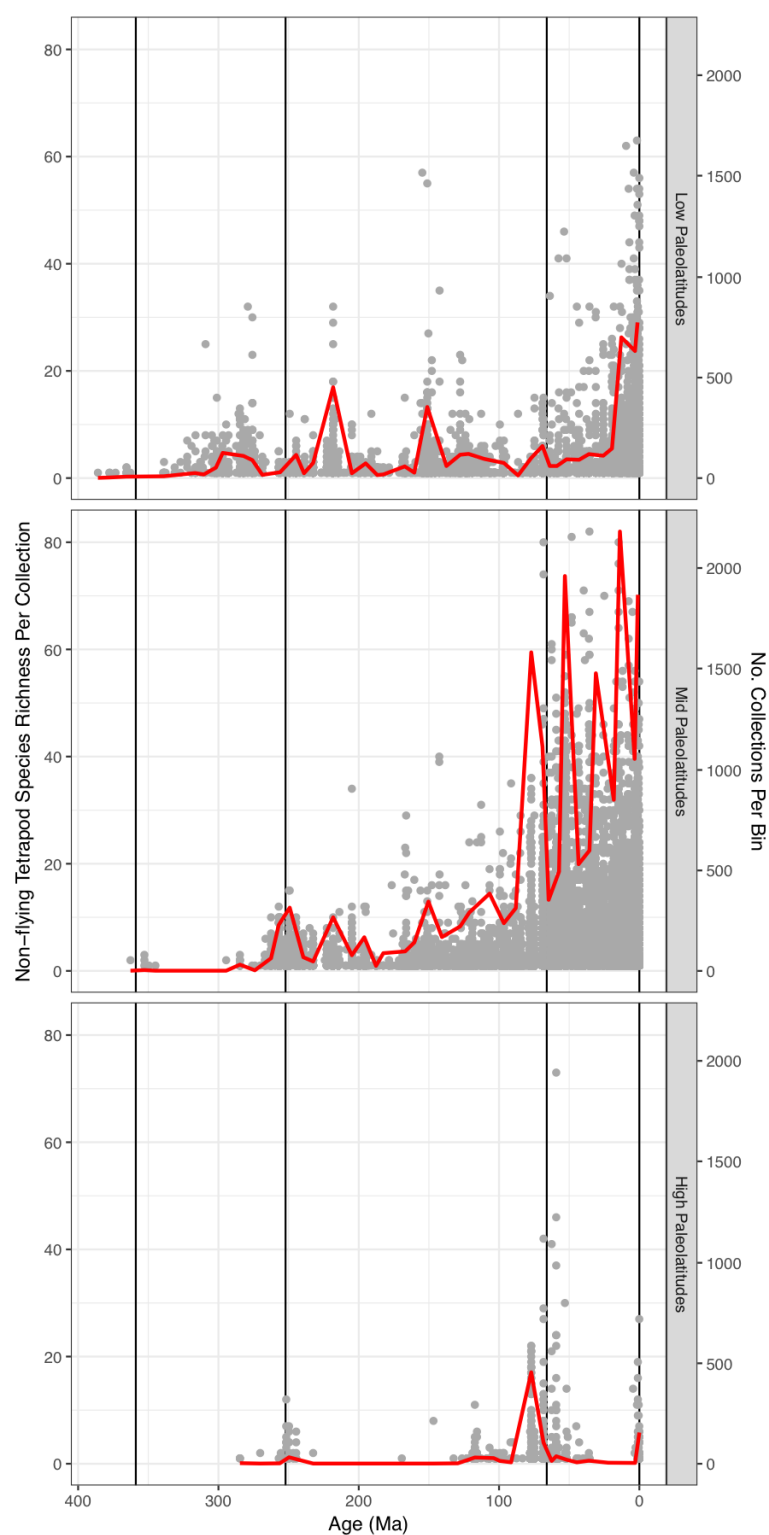
**Supplementary Fig. 16.** Paleolatitudes of collections through time, highlighting dominance of paleotemperate records and substantial increases in geographic coverage through time. Color range represents non-flying terrestrial tetrapod local richness. Black circles indicate exceptional localities.



**Supplementary Fig. 17.** Patterns of local richness in Phanerozoic non-flying tetrapods for key continental regions defined in the Methods section.



**Supplementary Fig. 18. Local species richness for less diverse tetrapod groups, superimposed against the pattern for all non-flying tetrapods. Species per collection for a, Pseudosuchians. b, Turtles. c, Lissamphibians. Species per formation for d, Pseudosuchians. e, Turtles. f, Lissamphibians.**



**Supplementary Fig. 19.** Patterns of local richness within paleolatitudinal belts (low = 0–30°, mid = 30–60°, high = 60–90°). Red line indicates number of collections per equal-length bin.

## Supplementary Tables

Superlocality Set	Model	Adj. R-Squared	p-value	df	AIC	Akaike Weights	p-value (Time)	coef. (Time)	p-value (Phase)	coef. (Phase 3)	p-value (Phase)	coef. (Phase 4)
None 0.99	~ Time +	0.689	< 0.001	4	44.509	0.541	< 0.001	-0.002	< 0.001	-0.452	< 0.001	-0.744
	~ Time *	0.691	< 0.001	6	44.875	0.408	< 0.001	-0.001	< 0.001	-0.329	0.002	-1.188
	~ Phase	0.681	< 0.001	3	49.322	0.051	-	-	< 0.001	-0.566	< 0.001	-1.096
	~ Time	0.641	< 0.001	2	140.781	0	< 0.001	-0.005	-	-	-	-
	~ 1	0	-	1	380.663	0	-	-	-	-	-	-
	Pg0-Ng4	-0.036	0.9	2	-	-	-	-	-	-	-	-
	Tr4-K8	0.219	< 0.001	2	-	-	-	-	-	-	-	-
None 0.995	C4-Tr5	0.002	0.27	2	-	-	-	-	-	-	-	-
	~ Phase	0.679	< 0.001	3	5.664	0.645	-	-	< 0.001	-0.509	< 0.001	-0.995
	~ Time +	0.679	< 0.001	4	6.959	0.314	< 0.001	-0.001	< 0.001	-0.466	< 0.001	-0.851
	~ Time *	0.674	< 0.001	6	10.625	0.041	< 0.001	-0.001	< 0.001	-0.5	0.21	-0.625
	~ Time	0.624	< 0.001	2	95.412	0	< 0.001	-0.005	-	-	-	-
	~ 1	0	-	1	209.887	0	-	-	-	-	-	-
	Pg0-Ng4	-0.052	0.59	2	-	-	-	-	-	-	-	-
None 0.998	Tr4-K8	0.114	0.012	2	-	-	-	-	-	-	-	-
	C4-Tr5	-0.006	0.42	2	-	-	-	-	-	-	-	-
	~ Phase	0.766	< 0.001	3	-20.037	0.705	-	-	< 0.001	-0.312	< 0.001	-0.944
	~ Time +	0.762	< 0.001	4	-18.416	0.255	< 0.001	0.001	< 0.001	-0.347	< 0.001	-1.064
	~ Time *	0.759	< 0.001	6	-15.949	0.041	< 0.001	0	0.055	-0.293	0.003	-1.568
	~ Time	0.673	< 0.001	2	59.059	0	< 0.001	-0.006	-	-	-	-
	~ 1	0	-	1	110.663	0	-	-	-	-	-	-
Moderate 0.99	Pg0-Ng4	-0.021	0.39	2	-	-	-	-	-	-	-	-
	Tr4-K8	0.412	0.002	2	-	-	-	-	-	-	-	-
	C4-Tr5	-0.044	0.89	2	-	-	-	-	-	-	-	-
	~ Time +	0.54	< 0.001	4	28.74	0.712	< 0.001	-0.002	< 0.001	-0.43	0.33	-0.185
	~ Time *	0.539	< 0.001	6	31.176	0.181	< 0.001	0	0.004	-0.325	0.72	-0.204
	~ Phase	0.526	< 0.001	3	32.647	0.107	-	-	< 0.001	-0.558	< 0.001	-0.59
	~ Time	0.343	< 0.001	2	82.34	0	< 0.001	-0.003	-	-	-	-
Moderate 0.995	~ 1	0	-	1	146.992	0	-	-	-	-	-	-
	Pg0-Ng4	0.113	0.2	2	-	-	-	-	-	-	-	-
	Tr4-K8	0.019	0.14	2	-	-	-	-	-	-	-	-
	C4-Tr5	-0.01	0.68	2	-	-	-	-	-	-	-	-
	~ Phase	0.598	< 0.001	3	-6.119	0.718	-	-	< 0.001	-0.487	< 0.001	-0.731
	~ Time +	0.593	< 0.001	4	-4.226	0.251	< 0.001	0	< 0.001	-0.469	0.002	-0.67
	~ Time *	0.585	< 0.001	6	-0.647	0.031	< 0.001	-0.001	< 0.001	-0.519	0.46	-0.415
Moderate 0.995	~ Time	0.4	< 0.001	2	25.755	0	< 0.001	-0.003	-	-	-	-
	~ 1	0	-	1	66.682	0	-	-	-	-	-	-
Moderate 0.995	Pg0-Ng4	0.001	0.35	2	-	-	-	-	-	-	-	-

	Tr4-K8	-0.004	0.36	2	-	-	-	-	-	-	-	-
	C4-Tr5	-0.019	0.63	2	-	-	-	-	-	-	-	-
Moderate 0.998	~ Phase	0.737	< 0.001	3	-20.991	0.684	-	-	< 0.001	-0.332	< 0.001	-0.825
	~ Time +	0.734	< 0.001	4	-19.716	0.276	< 0.001	-0.001	0.002	-0.283	0.009	-0.65
	~ Time *	0.722	< 0.001	6	-16.474	0.024	< 0.001	-0.002	0.018	-0.384	0.29	-0.616
	~ Time	0.662	< 0.001	2	-12.951	0.015	< 0.001	-0.003	-	-	-	-
	~ 1	0	-	1	25.187	0	-	-	-	-	-	-
	Pg0-Ng4	0.015	0.38	2	-	-	-	-	-	-	-	-
	Tr4-K8	0.154	0.082	2	-	-	-	-	-	-	-	-
	C4-Tr5	0.092	0.12	2	-	-	-	-	-	-	-	-
Stringent 0.99	~ Time +	0.519	< 0.001	4	40.837	0.544	< 0.001	-0.001	< 0.001	-0.467	0.2	-0.29
	~ Phase	0.511	< 0.001	3	41.737	0.373	-	-	< 0.001	-0.574	< 0.001	-0.629
	~ Time *	0.513	< 0.001	6	44.182	0.083	< 0.001	0	0.003	-0.393	0.71	-0.237
	~ Time	0.31	< 0.001	2	80.968	0	< 0.001	-0.003	-	-	-	-
	~ 1	0	-	1	123.415	0	-	-	-	-	-	-
	Pg0-Ng4	0.113	0.2	2	-	-	-	-	-	-	-	-
	Tr4-K8	0.003	0.28	2	-	-	-	-	-	-	-	-
	C4-Tr5	-0.019	0.88	2	-	-	-	-	-	-	-	-
Stringent 0.995	~ Phase	0.579	< 0.001	3	0.624	0.716	-	-	< 0.001	-0.475	< 0.001	-0.74
	~ Time +	0.574	< 0.001	4	2.438	0.255	< 0.001	0	< 0.001	-0.449	0.006	-0.653
	~ Time *	0.563	< 0.001	6	6.055	0.029	< 0.001	-0.001	< 0.001	-0.504	0.46	-0.432
	~ Time	0.407	< 0.001	2	23.743	0	< 0.001	-0.003	-	-	-	-
	~ 1	0	-	1	59.309	0	-	-	-	-	-	-
	Pg0-Ng4	0.001	0.35	2	-	-	-	-	-	-	-	-
	Tr4-K8	0.005	0.29	2	-	-	-	-	-	-	-	-
	C4-Tr5	-0.021	0.54	2	-	-	-	-	-	-	-	-
Stringent 0.998	~ Phase	0.739	< 0.001	3	-15.451	0.74	-	-	< 0.001	-0.355	< 0.001	-0.848
	~ Time +	0.732	< 0.001	4	-13.753	0.232	< 0.001	-0.001	0.003	-0.319	0.009	-0.725
	~ Time	0.653	< 0.001	2	-7.259	0.015	< 0.001	-0.003	-	-	-	-
	~ Time *	0.713	< 0.001	6	-9.951	0.014	< 0.001	-0.001	0.038	-0.367	0.33	-0.599
	~ 1	0	-	1	25.647	0	-	-	-	-	-	-
	Pg0-Ng4	0.015	0.38	2	-	-	-	-	-	-	-	-
	Tr4-K8	0.154	0.082	2	-	-	-	-	-	-	-	-
	C4-Tr5	-0.048	0.53	2	-	-	-	-	-	-	-	-

**Supplementary Table 1.** Relationships between species richness for Phanerozoic non-flying tetrapods within each of nine numerically-defined sets of exceptional localities (‘Superlocality Set’), and combinations of time and diversification phase (see Methods). Bottom three rows in each set of exceptional localities show models for regressions within individual diversification phases.

Bin	Stages	LAD	FAD	Midpoint	Duration
Ng4	Calabrian, Middle F	0	1.806	0.903	1.806
Ng3	Messinian, Zanclean	1.806	7.246	4.526	5.44
Ng2	Langhian, Serravalle	7.246	15.97	11.608	8.724
Ng1	Aquitanian, Burdigala	15.97	23.03	19.5	7.06
Pg5	Chattian, Rupelian	23.03	33.9	28.465	10.87
Pg4	Bartonian, Priabonian	33.9	41.3	37.6	7.4
Pg3	Lutetian	41.3	47.8	44.55	6.5
Pg2	Ypresian	47.8	56	51.9	8.2
Pg1	Selandian, Thanetian	56	61.6	58.8	5.6
Pg0	Danian	61.6	66	63.8	4.4
K8	Maastrichtian	66	72.1	69.05	6.1
K7	Campanian	72.1	83.6	77.85	11.5
K6	Coniacian, Santonian	83.6	93.9	88.75	10.3
K5	Cenomanian	93.9	100.5	97.2	6.6
K4	Albian	100.5	113	106.75	12.5
K3	Aptian	113	125	119	12
K2	Barremian, Hauterivian	125	132.9	128.95	7.9
K1	Berriasian, Valanginian	132.9	145	138.95	12.1
J6	Kimmeridgian, Tithonian	145	157.3	151.15	12.3
J5	Calloviaian, Oxfordian	157.3	166.1	161.7	8.8
J4	Bajocian, Bathonian	166.1	170.3	168.2	4.2
J3	Aalenian, Toarcian	170.3	182.7	176.5	12.4
J2	Pliensbachian	182.7	190.8	186.75	8.1
J1	Hettangian, Sinemurian	190.8	201.3	196.05	10.5
Tr5	Rhaetian	201.3	208.5	204.9	7.2
Tr4	Norian	208.5	228	218.25	19.5
Tr3	Carnian	228	237	232.5	9
Tr2	Ladinian	237	242	239.5	5
Tr1	Anisian, Olenekian	242	252.17	247.085	10.17
P5	Changhsingian, Wuchiapinguan	252.17	259.9	256.035	7.73
P4	Capitanian, Wordian	259.9	268.8	264.35	8.9
P3	Kungurian, Roadian	268.8	279.3	274.05	10.5
P2	Artinskian	279.3	290.1	284.7	10.8
P1	Asselian, Sakmarian	290.1	298.9	294.5	8.8
C5	Gzhelian, Kasimovian	298.9	307	302.95	8.1
C4	Moscovian	307	315.2	311.1	8.2
C3	Bashkirian, Serpukhovian	315.2	330.9	323.05	15.7
C2	Visean	330.9	346.7	338.8	15.8
C1	Tournaisian	346.7	358.9	352.8	12.2
D5	Famennian	358.9	372.2	365.55	13.3
D4	Frasnian	372.2	382.7	377.45	10.5

371

372 **Supplementary Table 2.** Definitions of approximately equal-length time bins.

373



Coll No	Coll Name	Formation	Period	Stage	Country	Geographic Scale	Stratigraphic Scale	Specimen Count	Sampling Level	Body-Size Range	Bulk Sampling	Environment	Lithology
18284	Norden Bridge Quarry	Valentine	Cenozoic	Barstovian	US	local area	group of beds	4288	extensive	small-large	no	channel	sandstone
18442	Valentine Railway Quarries	Valentine	Cenozoic	Barstovian	US	local area	group of beds	2760	extensive	small-large	no	terrestrial indet.	
46955	Hambach mine horizon 6C	Ville	Cenozoic	MN 5	DE	local area	group of beds	1900	extensive	small-large	yes	paralic indet.	lignite
16919	Calf Creek	Cypress Hills	Cenozoic	Chadronian	CA	outcrop	group of beds	2900	extensive	small-large	no	terrestrial indet.	not reported
12840	Le Bretou		Cenozoic	Bartonian	FR	local area	bed	-	very extensive	small-large	yes	karst indet.	phosphorite
16207	Davis Ranch	Wind River	Cenozoic	Bridgerian	US	outcrop	group of beds	1490	extensive	small-large	unknown	fluvial-lacustrine indet.	mudstone
16228	Grizzly Buttes	Bridger	Cenozoic	Bridgerian	US	local area	group of beds	-	extensive	small-large	no	terrestrial indet.	not reported
14939	Cochrane 2	Paskapoo	Cenozoic	Ti1	CA	outcrop	group of beds	1700	extensive	small-large	no	fluvial-lacustrine indet.	siltstone
14519	Bushy Tailed Blowout	Lance	Mesozoic	Lancian	US	local area	bed	-	extensive	small-medium	yes	terrestrial indet.	shale
14549	Flat Creek 5	Hell Creek	Mesozoic	Lancian	US	outcrop	bed	217	very extensive	small-very large	yes	terrestrial indet.	sandstone

<b>14566</b>	Hatcher No. 2 (UCMP V-5815)	Lance	Mesozoic	Lancian	US	outcrop	bed	-	extensive	small- very large	yes	terrestrial indet.	sandstone
<b>14585</b>	Lull 2 Quarry (UCMP V-5620)	Lance	Mesozoic	Late Maastrichtian	US	outcrop	bed	-	extensive	small- very large	yes	terrestrial indet.	sandstone
<b>45726</b>	Ksar Met-Lili, Anoual	Ksar Metlili	Mesozoic	Berriasian	MA	outcrop	group of beds	-	extensive	small- very large	yes	deltaic indet.	limestone
<b>28401</b>	Sunnydown Farm Quarry	Lulworth	Mesozoic	Middle Berriasian	UK	outcrop	group of beds	26	extensive	small- medium	yes	lacustrine - small	limestone
<b>12816</b>	Quarry 9, Como Bluff (YPM)	Morrison	Mesozoic	Kimmeridgian- Tithonian	US	outcrop	bed	3748	very extensive	small- very large	yes	fluvial- lacustrine indet.	mudstone
<b>24563</b>	Guimarota	Alcobaça	Mesozoic	Kimmeridgian	PT	local area	group of beds	-	very extensive	small- very large	yes	lagoonal	coal
<b>39075</b>	Kirtlington 3p (Mammal Bed)	Forest Marble	Mesozoic	Late Bathonian	UK	outcrop	bed	1590	extensive	small- very large	yes	mire/swamp	marl
<b>24883</b>	Dashanpu Dinosaur Quarry	Xiashaximiao	Mesozoic	Bajocian - Callovian	CN	outcrop	bed	-	extensive	medium- very large	no	lacustrine indet.	sandstone
<b>39160</b>	Placerias Quarry, UCMP A269	Chinle	Mesozoic	Norian	US	outcrop	group of beds	-	very extensive	small- large	yes	wet floodplain	mudstone
<b>86388</b>	Abrahamskraal, Prince Albert	Abrahamskraal	Palaeozoic	Cap	ZA	local area	group of beds	33	very extensive	medium	no	floodplain	sandstone
<b>28256</b>	Coffee Creek, 34	Arroyo	Palaeozoic	Kun	US	local area	formation	50	very extensive	small- large	no	terrestrial indet.	claystone

<b>28267</b>	Craddock Bonebed, Brush Creek, 38	Arroyo	Palaeozoic	Kun	US	local area	group of beds	61	very extensive	small-large	no	terrestrial indet.	claystone
<b>67862</b>	Richards Spur	Garber	Palaeozoic	Leo	US	local area	formation	320	very extensive	small-large	no	fissure fill	claystone
<b>84835</b>	Nyrany	Kladno	Palaeozoic	West D	CZ	local area	formation	38	very extensive	small-medium	yes	lacustrine indet.	coal
<b>85292</b>	Linton		Palaeozoic	West D	US	outcrop	bed	69	very extensive	small-large	yes	mire/swamp	coal

375 **Supplementary Table 3.** Key information about selected exceptional localities yielding Phanerozoic terrestrial tetrapods.

